Nuclear physics across energy scales

Imaging shapes of atomic nuclei from large to small via flow measurement

Chunjian Zhang

Fudan University

September 18-21, 2025, Wuhan

Central China
Center for Nuclear Theory
华中核理论中心

Outline

I. Nuclear structure across energy scales

II. v_n and v_n-p_T correlation ($n \geq 2$) measurements in ^{238}U, ^{96}Zr and ^{16}O

III. New radial flow $v_0(p_T)$ measurement in ^{197}Au and ^{16}O

IV. Conclusions and outlooks

Shape of atomic nuclei

Emergent phenomena of the many-body quantum system, govern by short-range strong nuclear force

- Quadrupole/octupole/hexadecapole deformations
- Clustering, halo, skin, bubble…
- Non-monotonic evolution with *N* and *Z*

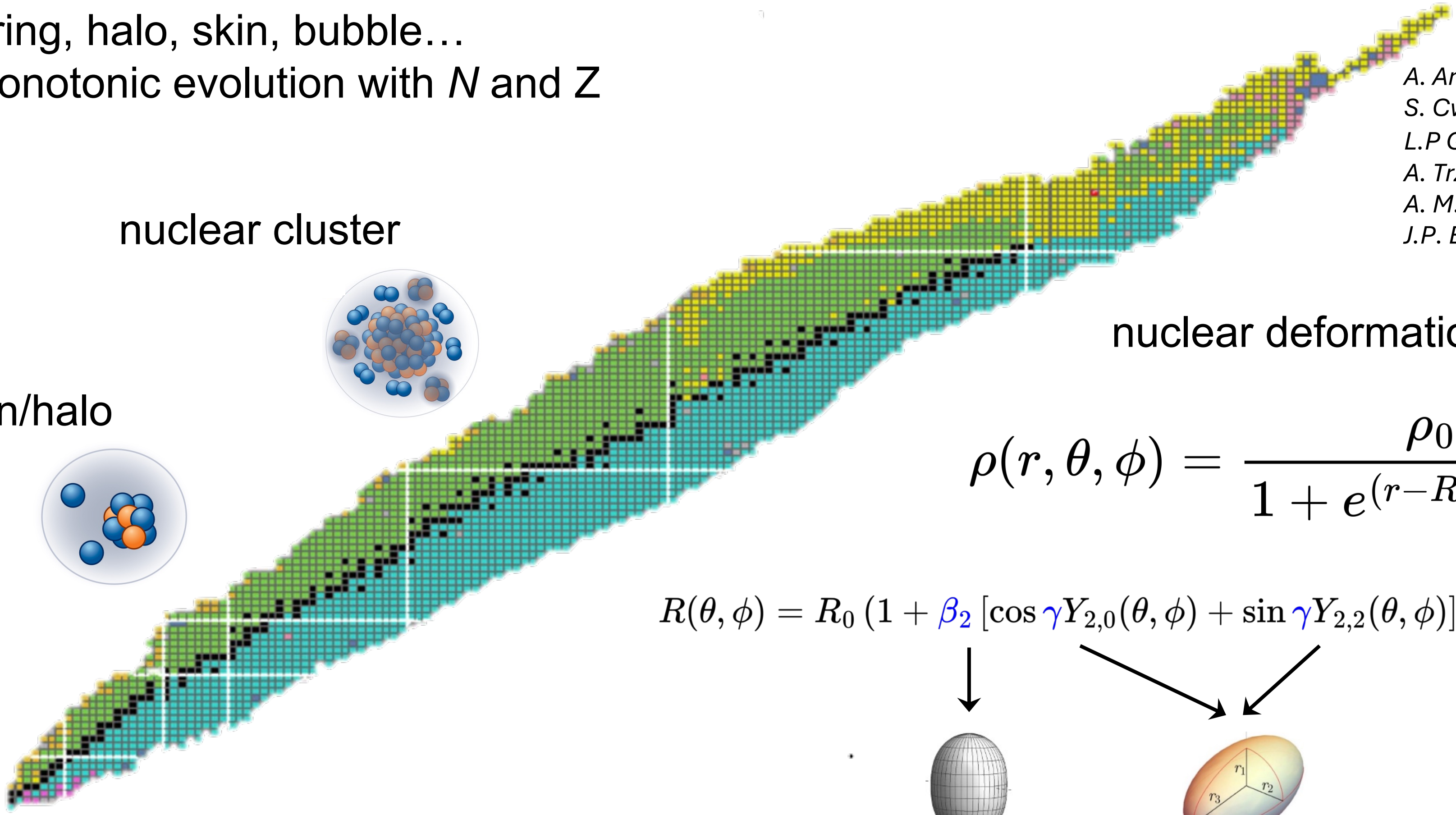

nuclear cluster

neutron skin/halo

Z (proton numbers)

N (neutron numbers)

A. Andreyev et al., Nature 405, 430 (2000)
S. Cwiok et al.,Nature 433, 705 (2005)
L.P Gaffney P. Butler et al., Nature 497, 199 (2013)
A. Trzcinska et al., PRL 87, 082501 (2001)
A. M. Centelles et al., PRL 102, 122502 (2009)
J.P. Ebran et al. Nature 487, 341 (2012)

nuclear deformation

$$\rho(r,\theta,\phi) = \frac{\rho_0}{1+e^{(r-R(\theta,\phi))/a_0}}$$

$$R(\theta,\phi) = R_0\left(1+\beta_2\left[\cos\gamma Y_{2,0}(\theta,\phi)+\sin\gamma Y_{2,2}(\theta,\phi)\right]+\beta_3 Y_{3,0}(\theta,\phi)+\beta_4 Y_{4,0}(\theta,\phi)\right)$$

Very rich landscape of shapes and other structures

Y. Ye, X. Yang, H. Sakurai, B. Hu, Nature Review Physics, 7, 21-37 (2025); Y. Ma, S. Zhang, Handbook of Nuclear Physics (2022)

Nuclear shape at low energy: long exposure

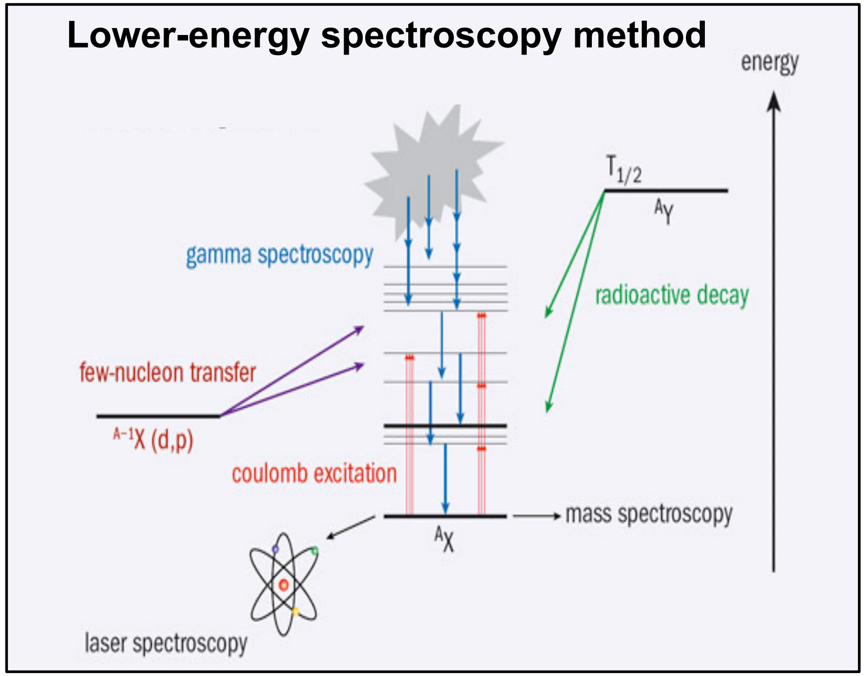

Traditional imaging method taken before destruction

→ Low energy spectroscopic methods probe a superposition of these fluctuations.
→ Instantaneous shapes not directly seen, but inferred from model comparison.

Each DOF has zero-point fluctuations within certain timescales.

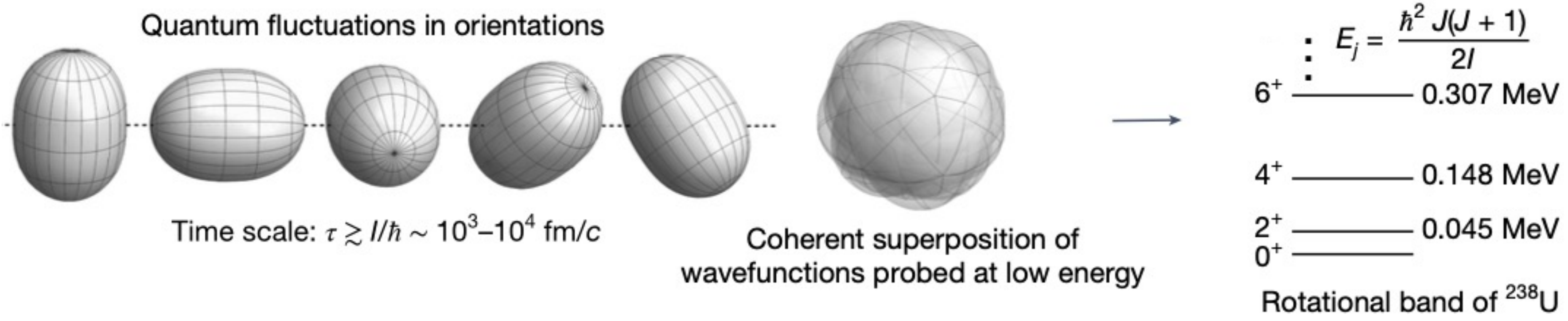

Imaging by smashing method

Take a snapshot

Evolution

Measurement

Nuclei collisions

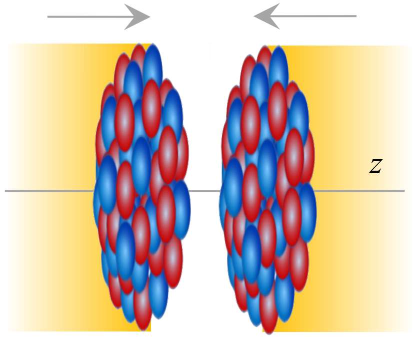

$T_{\mu\nu}(\tau = 0)$

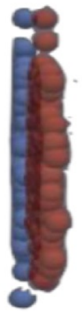

$\tau \sim 2R_0/\Gamma \sim 0.1\mathrm{fm}/c$

exposure

$\partial_\mu T^{\mu\nu} = 0$, EOS, viscosity…

Pressure-driven expansion of

Quark-gluon plasma (QGP)

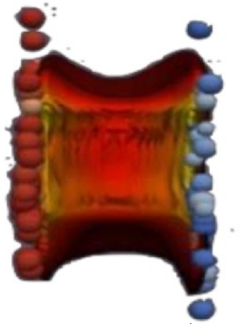

$\tau \sim 10\mathrm{fm}/c$

expansion

free-streaming

$T_{\mu\nu}(\tau = \infty)$

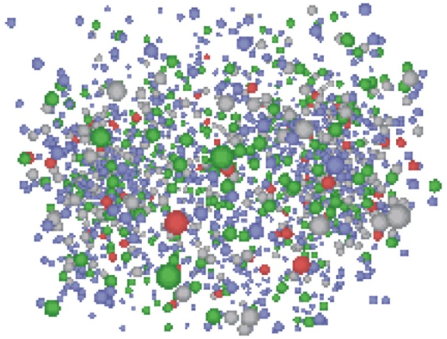

$\tau \sim 10^{15}\mathrm{fm}/c$

detection

$$\rho(r,\theta,\phi) = \frac{\rho_0}{1 + e^{(r - R(\theta,\phi))/a_0}}$$

- $\beta_2 \rightarrow$ quadrupole deformation
- $\beta_3 \rightarrow$ octupole deformation
- $\gamma \rightarrow$ triaxiality
- $a_0 \rightarrow$ surface diffuseness
- $R_0 \rightarrow$ nuclear size

ab initio theory/shell model/DFT

J. Jia et al., Nucl. Sci. Tech 35, 220 (2024)

Imaging by smashing method

Take a snapshot | Evolution | Measurement

Nuclei collisions

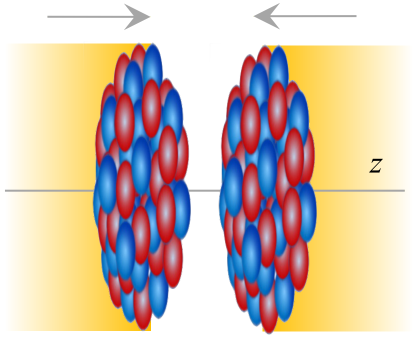

$T_{\mu\nu}(\tau = 0)$

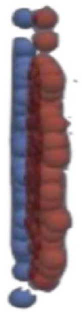

$\tau \sim 2R_0/\Gamma \sim 0.1\mathrm{fm}/c$
exposure

$\partial_\mu T^{\mu\nu} = 0$, EOS, viscosity…

Pressure-driven expansion of Quark-gluon plasma (QGP)

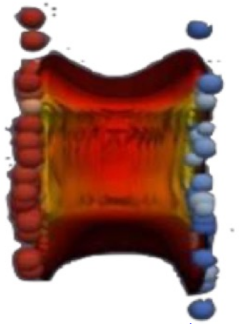

$\tau \sim 10\mathrm{fm}/c$
expansion

free-streaming

$T_{\mu\nu}(\tau = \infty)$

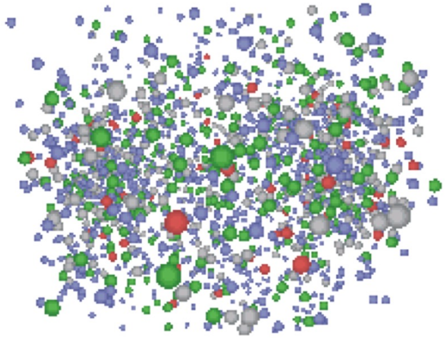

$\tau \sim 10^{15}\mathrm{fm}/c$
detection

$$\rho(r,\theta,\phi) = \frac{\rho_0}{1 + e^{(r-R(\theta,\phi))/a_0}}$$

- $\beta_2 \longrightarrow$ quadrupole deformation
- $\beta_3 \longrightarrow$ octupole deformation
- $\gamma \longrightarrow$ triaxiality
- $a_0 \longrightarrow$ surface diffuseness
- $R_0 \longrightarrow$ nuclear size

ab initio theory/shell model/DFT

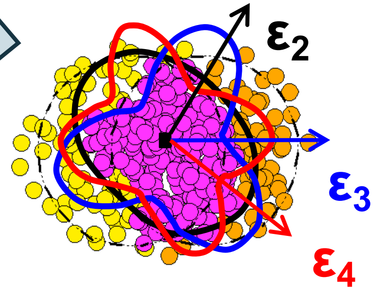

size & shape

J. Jia et al., Nucl. Sci. Tech 35, 220 (2024)

$R_\perp^2 \propto \langle r_\perp^2 \rangle$ $\quad \mathcal{E}_n \propto \langle r_\perp^n e^{in\phi} \rangle$

R_0 $\quad a_0$ $\quad \beta_n$

Observables $\frac{d^2N}{d\phi dp_T} = N(p_T)\left(\sum_n V_n e^{-in\phi}\right)$

Event-by-event linear responses:

$$\frac{\delta[p_T]}{[p_T]} \propto -\frac{\delta R_\perp}{R_\perp} \qquad V_n \propto \mathcal{E}_n$$

G. Giacalone et al., PRC 103, 024909 (2021); H. Niemi et al., PRC 87, 054901 (2013)

Key: 1) fast snapshot, 2) linear response, 3) large multiplicity for many-body correlation

Imaging nuclear shape in high-energy snapshot

- Nuclear shape in intrinsic (body-fixed) frame not directly visible in the lab frame

  --Mainly inferred from non-invasive spectroscopy methods.

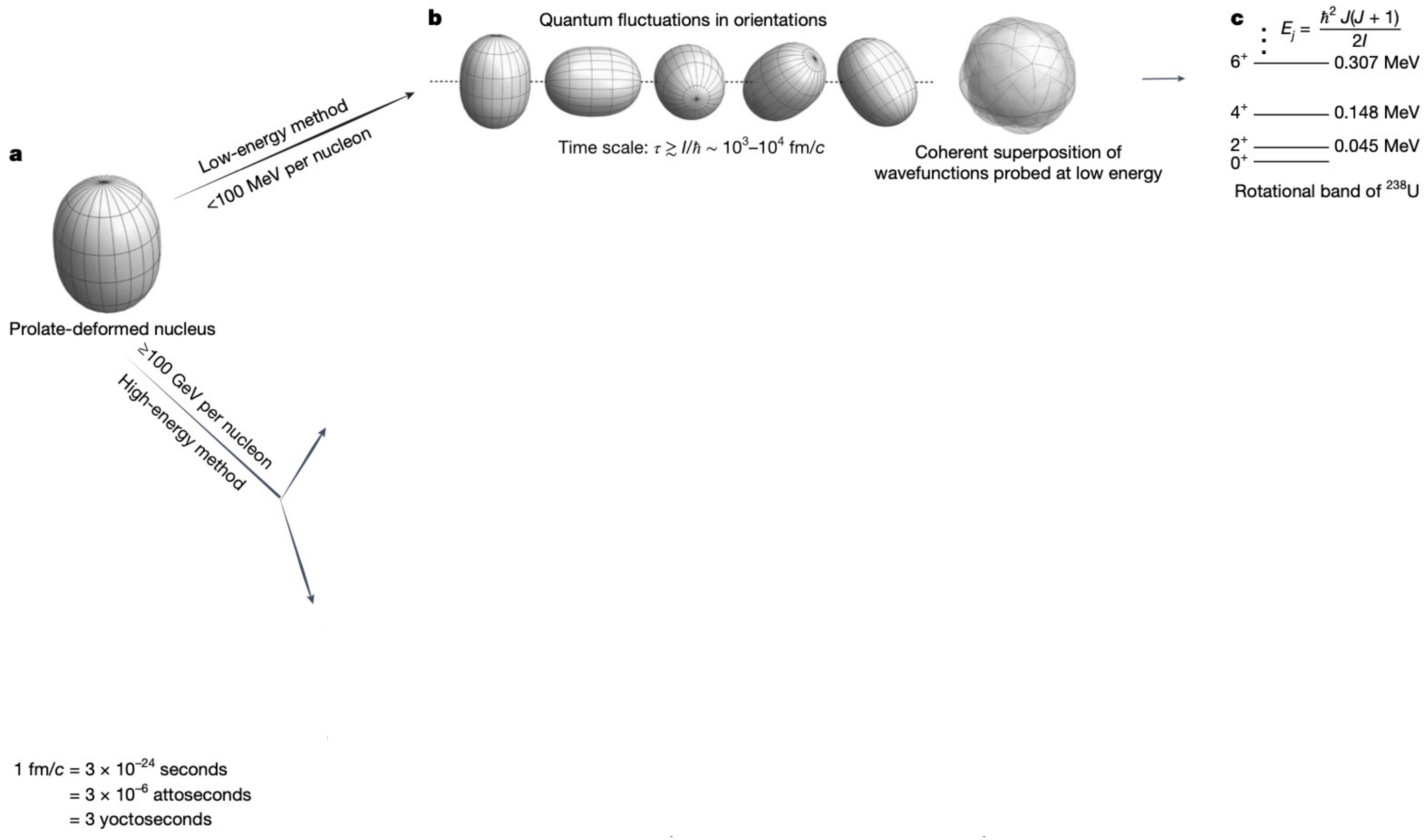

Imaging nuclear shape in high-energy snapshot

- Nuclear shape in intrinsic (body-fixed) frame not directly visible in the lab frame

  --Mainly inferred from non-invasive spectroscopy methods.

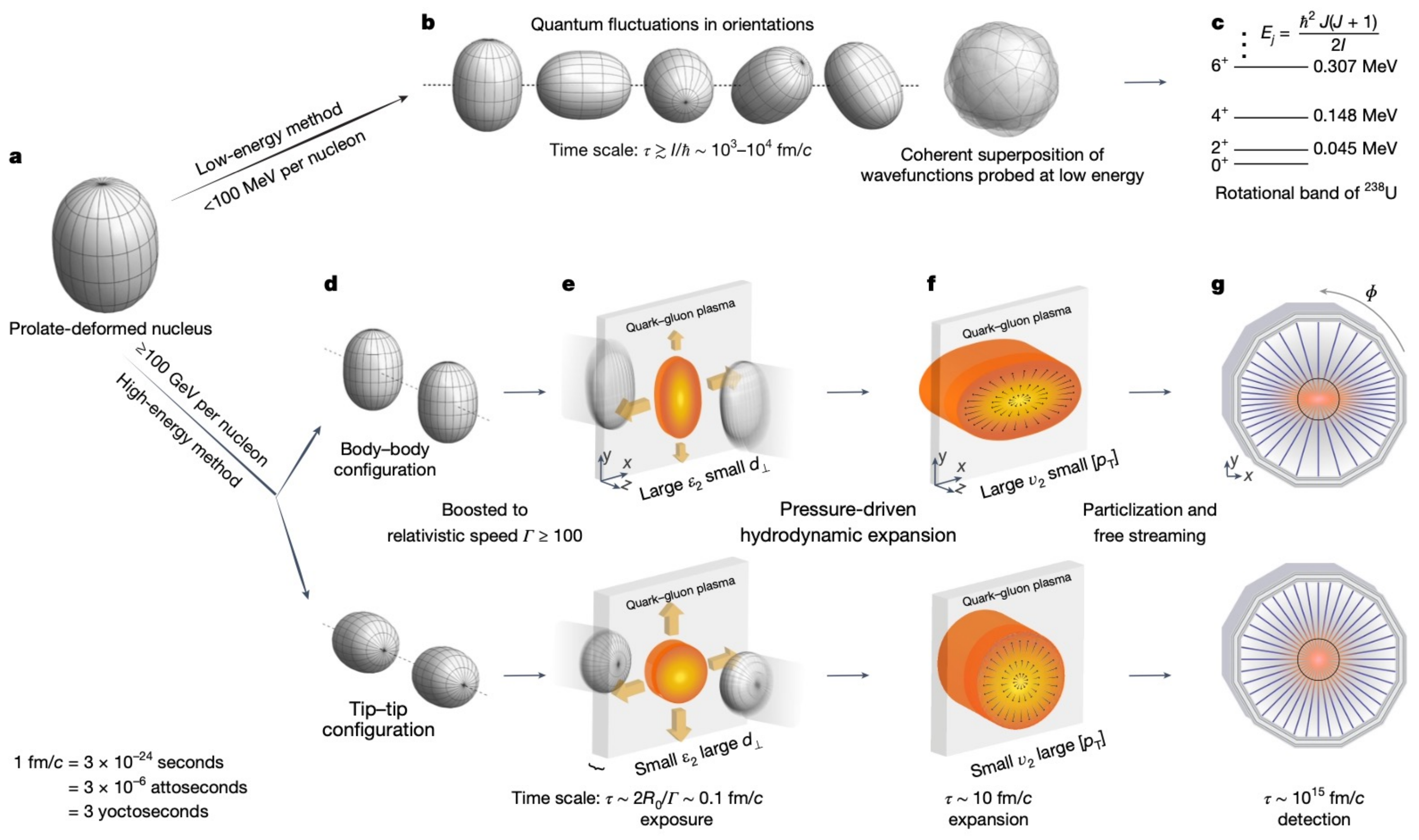

STAR, Nature 635, 67-72 (2024)

https://www.nature.com/articles/s41586-024-08097-2

Body-body: large-eccentricity large-size

$v_2\nearrow$ $p_T\searrow$

Tip-tip : small-eccentricity small-size

$v_2\searrow$ $p_T\nearrow$

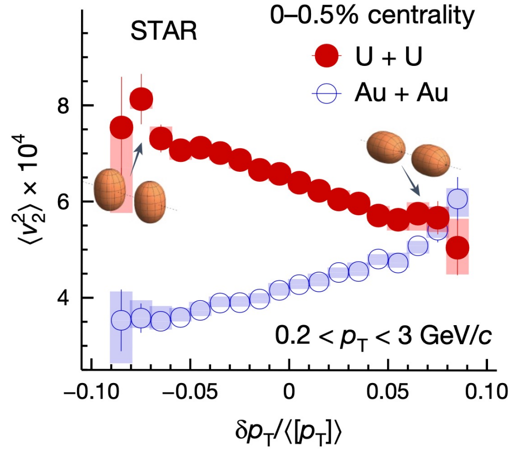

Imaging nuclear shape in high-energy snapshot

- Nuclear shape in intrinsic (body-fixed) frame not directly visible in the lab frame

  --Mainly inferred from non-invasive spectroscopy methods.

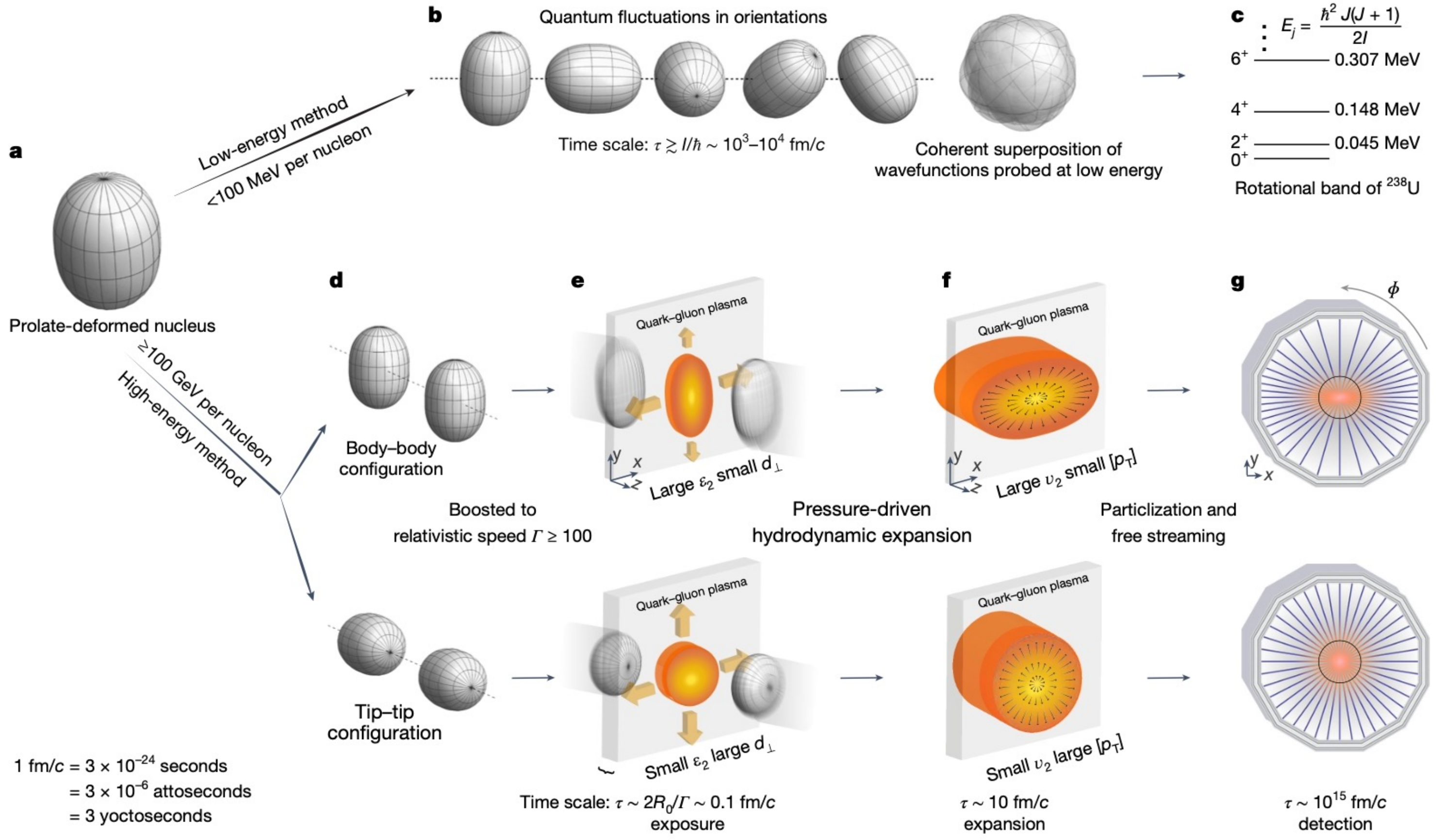

STAR, Nature 635, 67-72 (2024)
https://www.nature.com/articles/s41586-024-08097-2

across energy scales

Body-body: large-eccentricity large-size

$v_2\nearrow$ $p_T\searrow$

Tip-tip : small-eccentricity small-size

$v_2\searrow$ $p_T\nearrow$

$$\langle v_2^2\rangle = a_1 + b_1\beta_2^2,$$
$$\langle(\delta p_T)^2\rangle = a_2 + b_2\beta_2^2,$$
$$\langle v_2^2\delta p_T\rangle = a_3 - b_3\beta_2^3\cos(3\gamma).$$

G. Giacalone, J. Jia, C. Zhang, PRL 127, 242301(2021)

Shape-frozen like a snapshot during nuclear crossing (10^{-25}s << rotational time scale 10^{-21}s)

probe entire mass distribution in the intrinsic frame via multi-point correlations

Ratio of observables

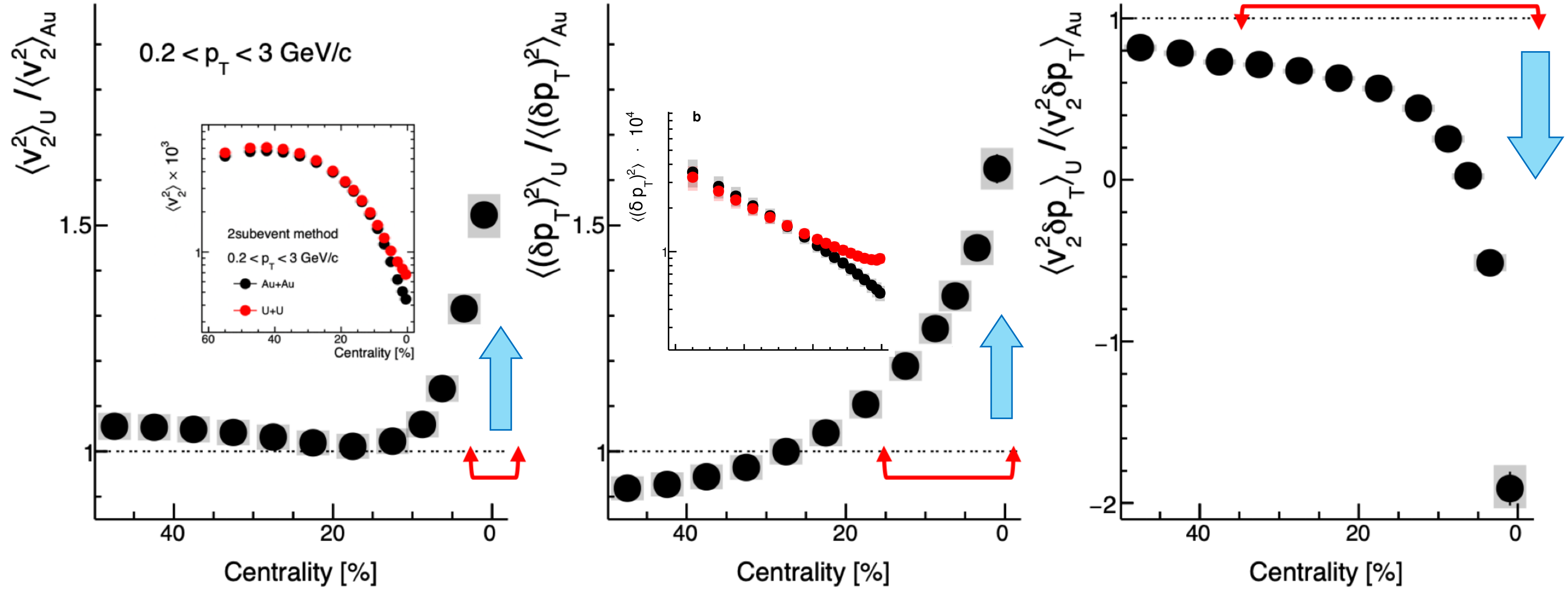

$$R_{\langle v_2^2\rangle} \approx 1 + \frac{b_1}{a_1}\beta_2^2,$$
$$R_{\langle(\delta p_T)^2\rangle} \approx 1 + \frac{b_2}{a_2}\beta_2^2,$$
$$R_{\langle v_2^2 \delta p_T\rangle} \approx 1 - \frac{b_3}{a_3}\beta_2^3 \cos(3\gamma)$$

- Elliptic flow and size fluctuation are enhanced by the nuclear deformation effect.
- Ratios cancel final state effects and isolate the effects of initial state/nuclear structures.

→ U deformation dominates the ultra-central collisions (UCC)

Constraining the ground-state ^{238}U: β_2 and γ

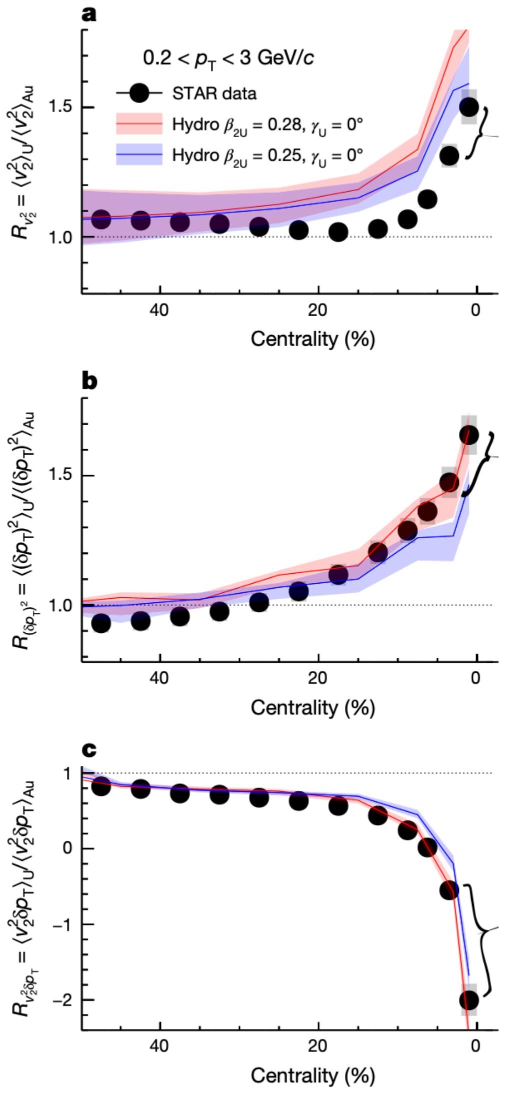

Constraining the ground-state ^{238}U: β_2 and γ

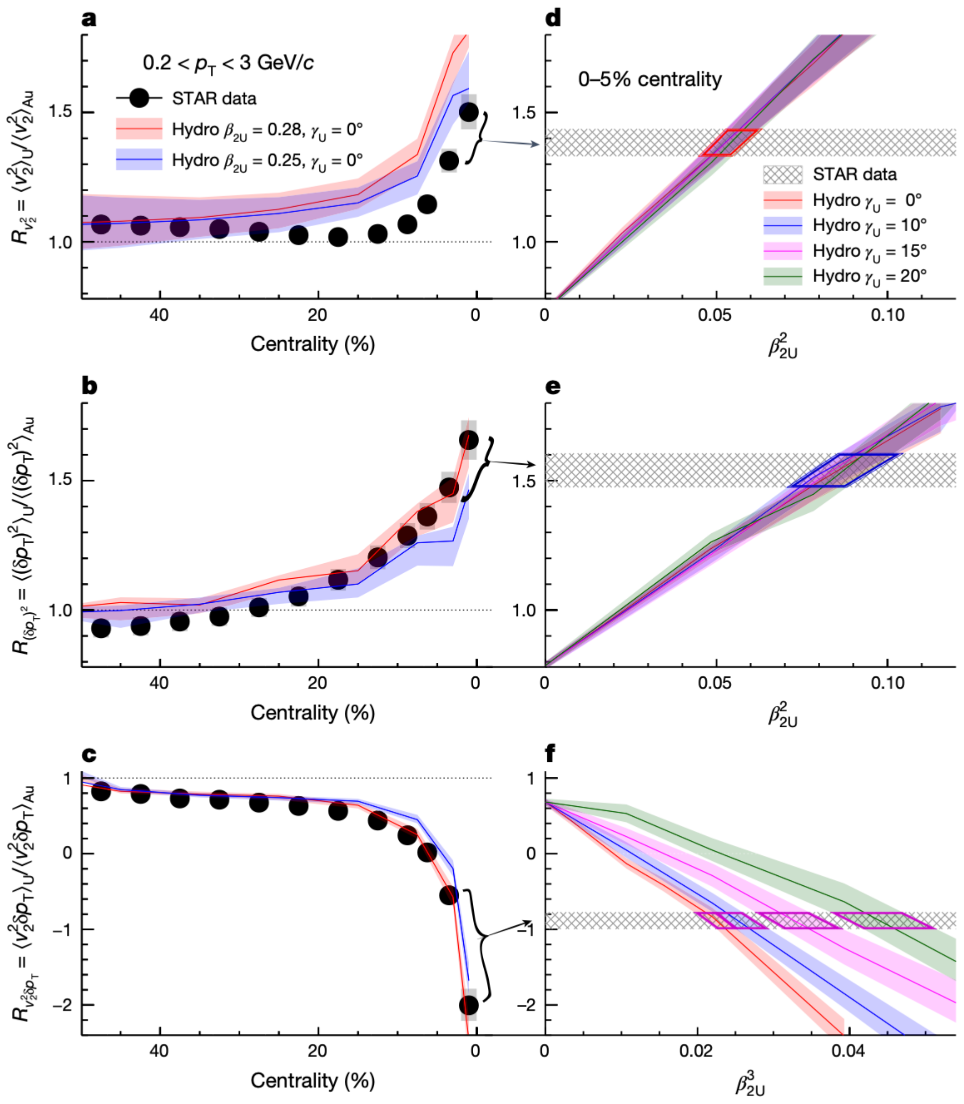

Sufficient precision is achieved from ratios in ultra-central collisions

Relation confirmed from hydro

$$R_{\langle v_2^2\rangle} \approx 1 + \frac{b_1}{a_1}\beta_2^2,$$
$$R_{\langle(\delta p_T)^2\rangle} \approx 1 + \frac{b_2}{a_2}\beta_2^2,$$
$$R_{\langle v_2^2 \delta p_T\rangle} \approx 1 - \frac{b_3}{a_3}\beta_2^3\cos(3\gamma)$$

Constraining the ground-state ^{238}U: β_2 and γ

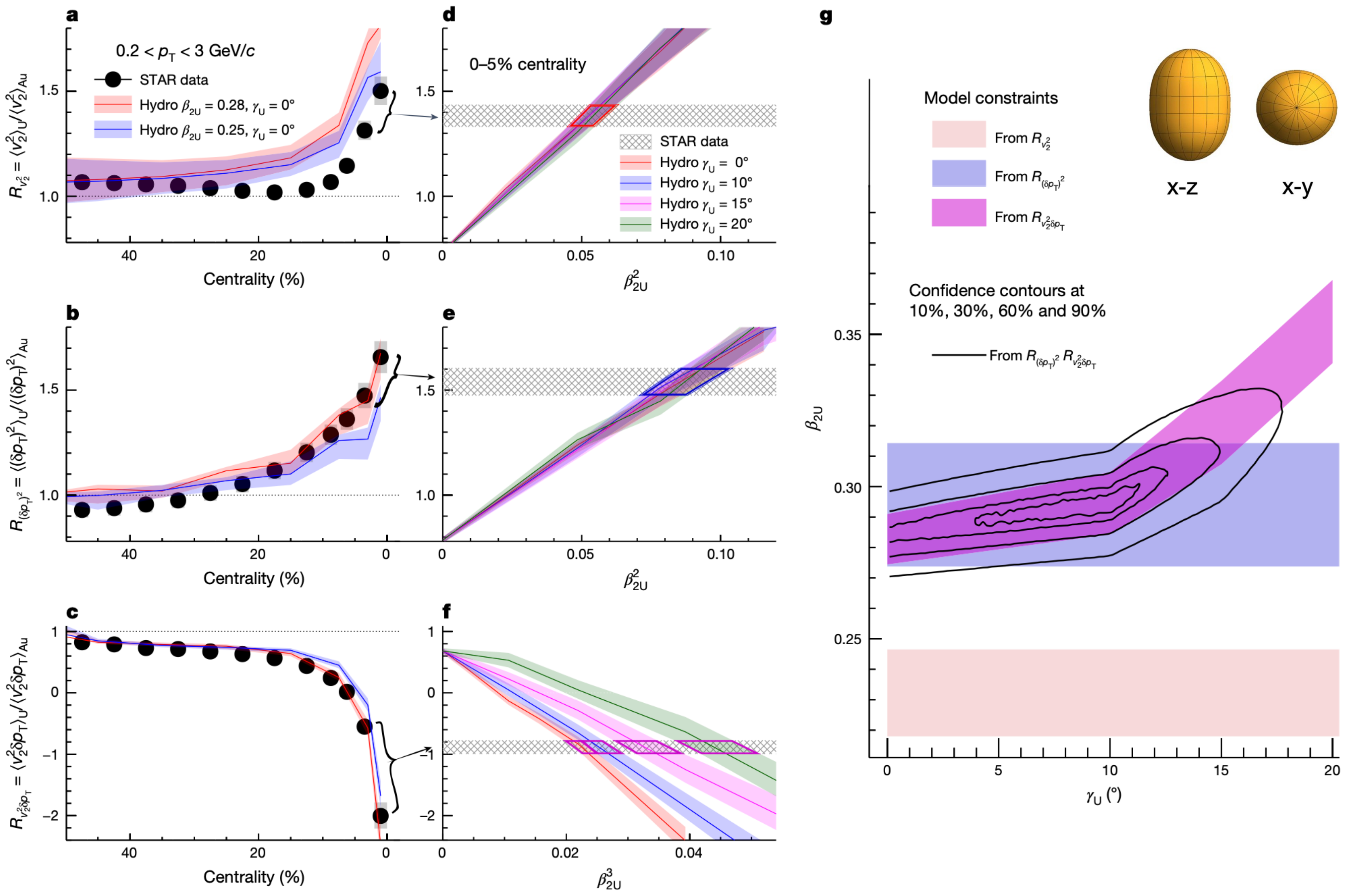

Sufficient precision is achieved from ratios in ultra-central collisions

Relation confirmed from hydro

$$R_{\langle v_2^2\rangle} \approx 1 + \frac{b_1}{a_1}\beta_2^2,$$
$$R_{\langle(\delta p_T)^2\rangle} \approx 1 + \frac{b_2}{a_2}\beta_2^2,$$
$$R_{\langle v_2^2 \delta p_T\rangle} \approx 1 - \frac{b_3}{a_3}\beta_2^3\cos(3\gamma)$$

High-energy estimate:

$$\beta_{2U} = 0.286 \pm 0.025$$
$$\gamma_U = 8.5^\circ \pm 4.8^\circ$$

low-energy estimate:

$$\beta_{2U} = 0.287 \pm 0.007$$
$$\gamma_U = 6^\circ - 8^\circ$$

A large deformation with a slight deviation from axial symmetry in the nuclear ground-state

Evidence of octupole deformation $\beta_{3,\mathrm{U}}$

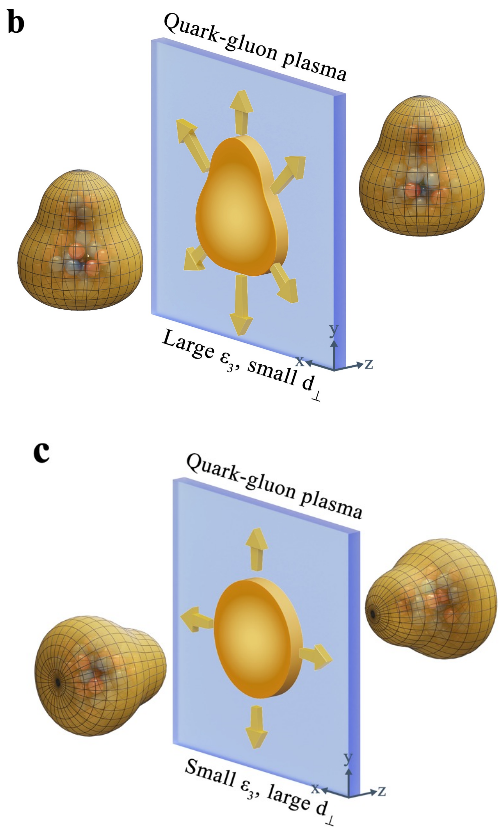

However, v_3 is fluctuation driven, expect in central

$$\langle v_3^2 \rangle \propto \langle \varepsilon_3^2 \rangle \sim 1/A$$

mass number

B. Alver and G. Roland, PRC 81, 054905 (2010)

Evidence of octupole deformation $\beta_{3,\mathrm{U}}$

IP-Glasma+MUSIC calculations

C. Zhang, J. Jia, J. Chen, C. Shen, L. Liu, arXiv: 2504.15245

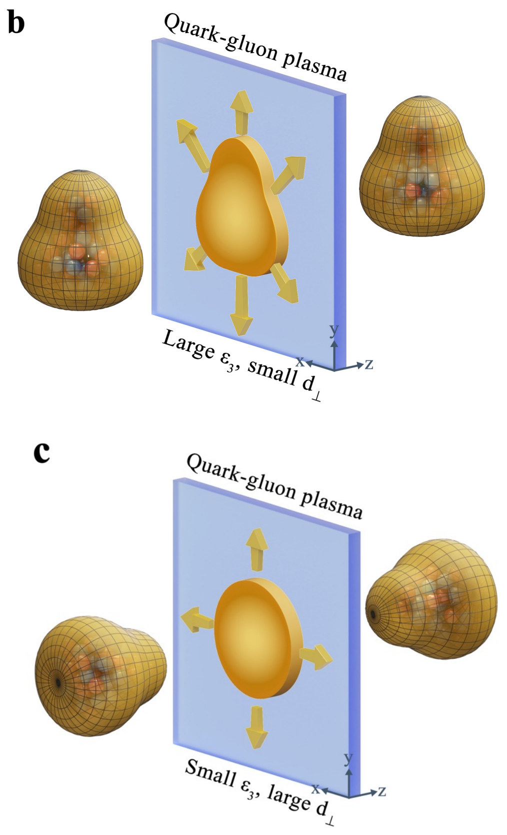

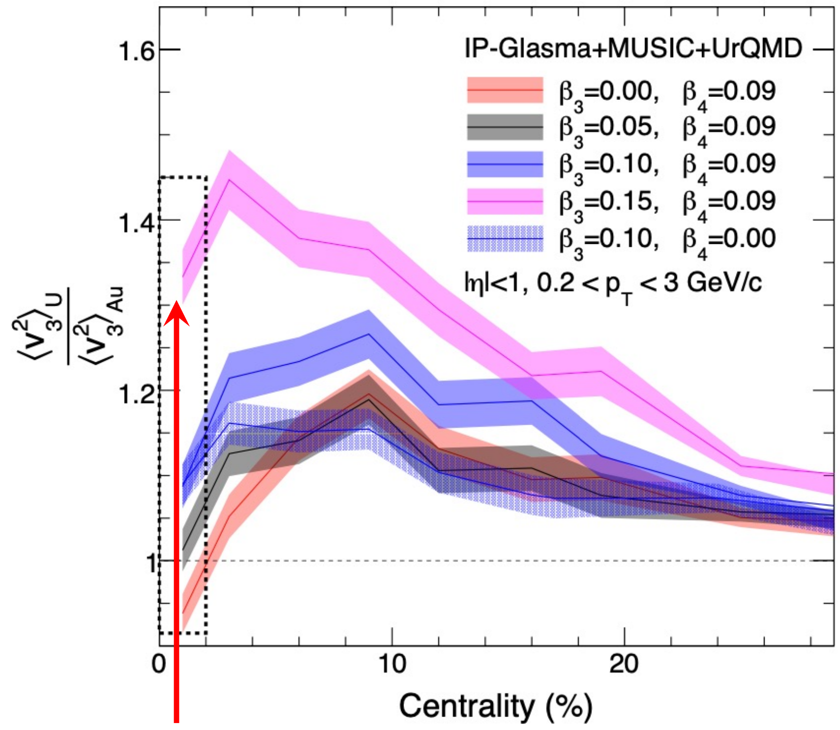

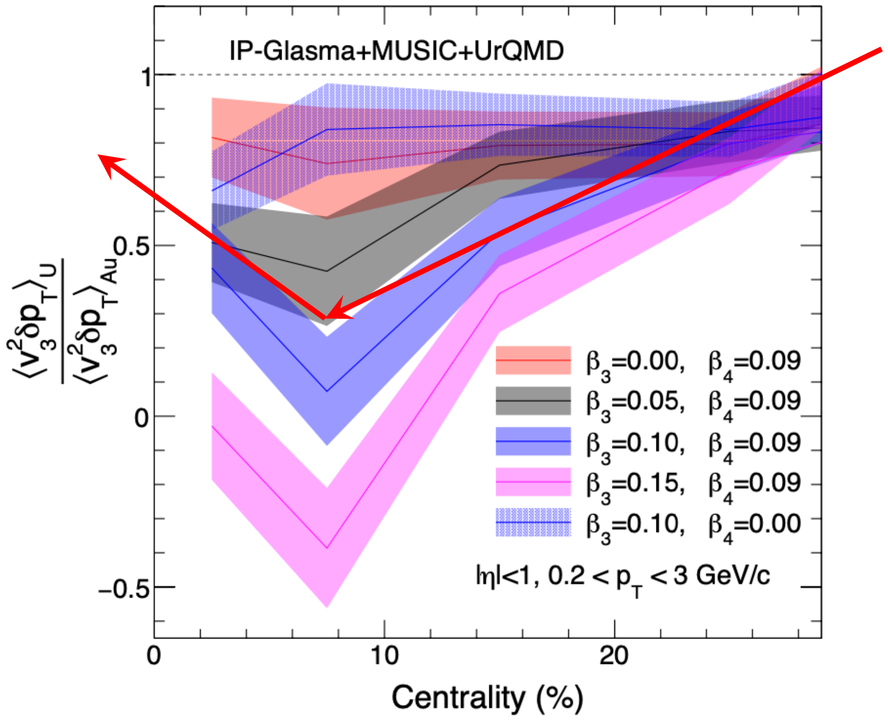

$$R_{v_3^2} = \frac{\langle v_3^2\rangle_{\mathrm{U+U}}}{\langle v_3^2\rangle_{\mathrm{Au+Au}}} \approx \frac{a_{3\mathrm{U}}}{a_{3\mathrm{Au}}} + \frac{b_{3,3}}{a_{3\mathrm{Au}}}\beta_3^2 + \frac{b_{3,4}}{a_{3\mathrm{Au}}}\beta_4^2,$$

$$R_{v_3^2\delta p_T} = \frac{\langle v_3^2\delta p_{\mathrm{T}}\rangle_{\mathrm{U+U}}}{\langle v_3^2\delta p_{\mathrm{T}}\rangle_{\mathrm{Au+Au}}} \approx a - b\beta_2\beta_3^2.$$

However, v_3 is fluctuation driven, expect in central

$$\langle v_3^2\rangle \propto \langle \varepsilon_3^2\rangle \sim 1/A$$

mass number

$\langle v_3^2\rangle$ follows a linear increase with β_3^2,

Characteristic anticorrelation in $\langle v_3^2\delta p_{\mathrm{T}}\rangle$ shows a pronounced β_3-dependent suppression.

B. Alver and G. Roland, PRC 81, 054905 (2010)

Evidence of octupole deformation $\beta_{3,U}$

New

STAR, arXiv: 2506.17785

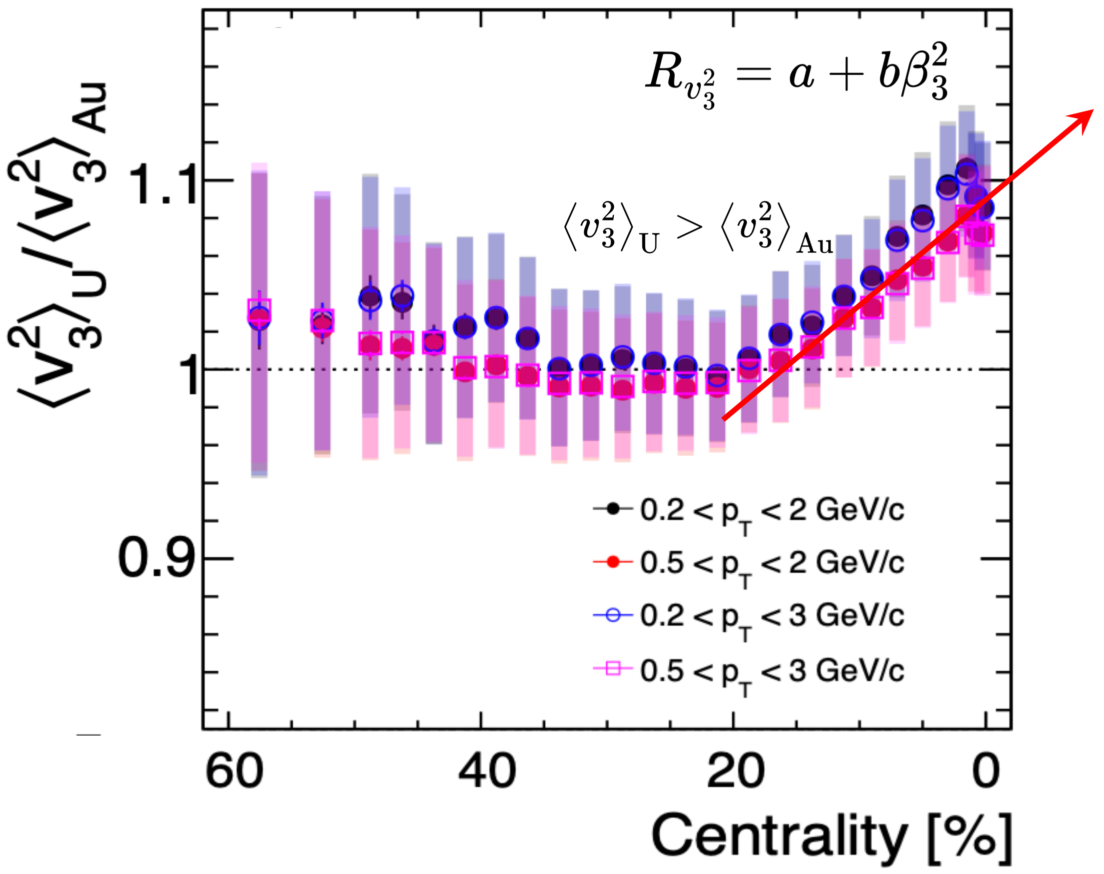

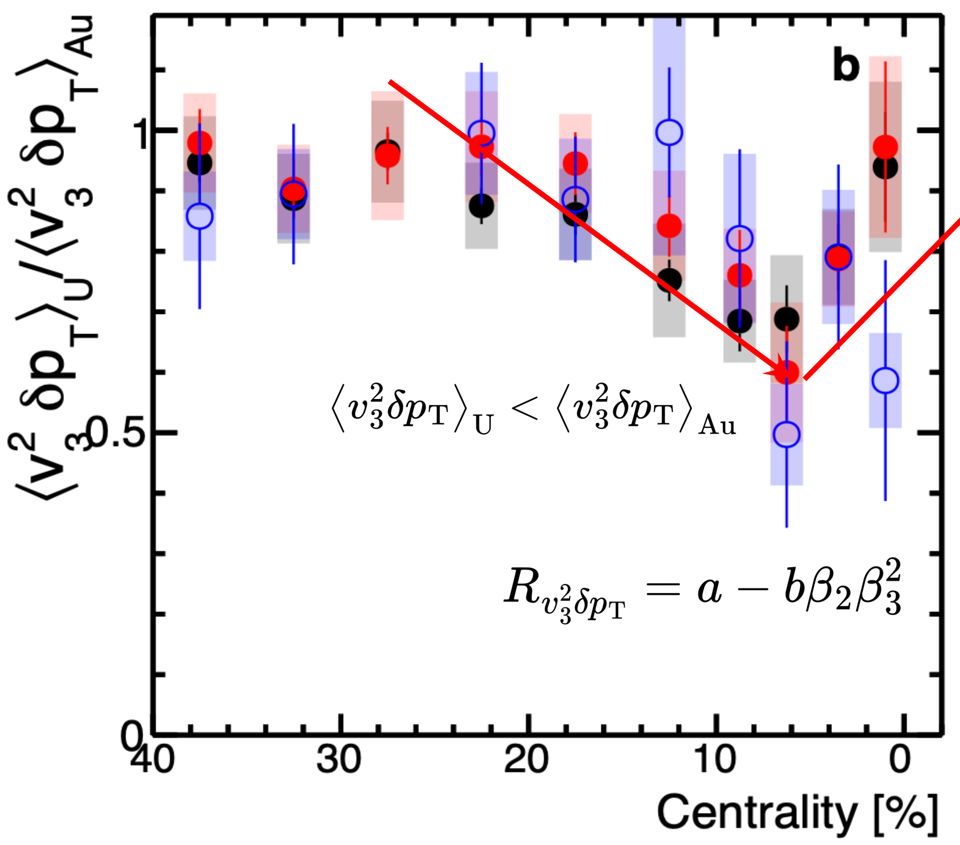

Order of v_3 and v_3-p_T reversed by considering non-zero $\beta_{3,U}$, $\beta_{4,U}$.

An evidence and modest $\beta_{3,U} \sim 0.08$-0.10 are confirmed.

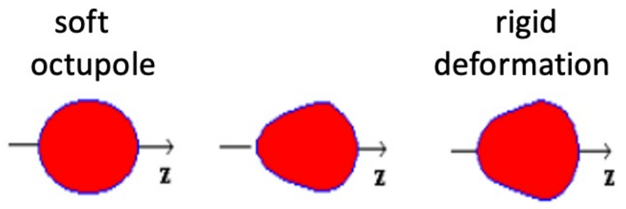

H. Xu, D. Xu, S. Zhao, W. Zhao, H. Song, F. Wang, 2504.19644; K. Hagino and M. Kitazawa, 2508.05125; *L. Liu, C. Zhang, J. Chen, J. Jia, X. Huang, Y. Ma, 2509.09376*

Nuclear structure via ^{96}Ru/^{96}Zr v_n ratio

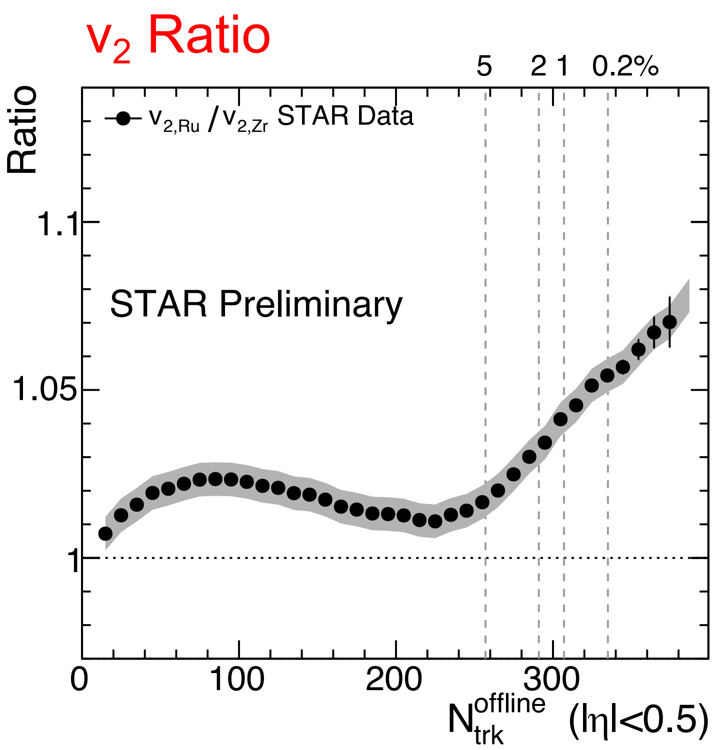

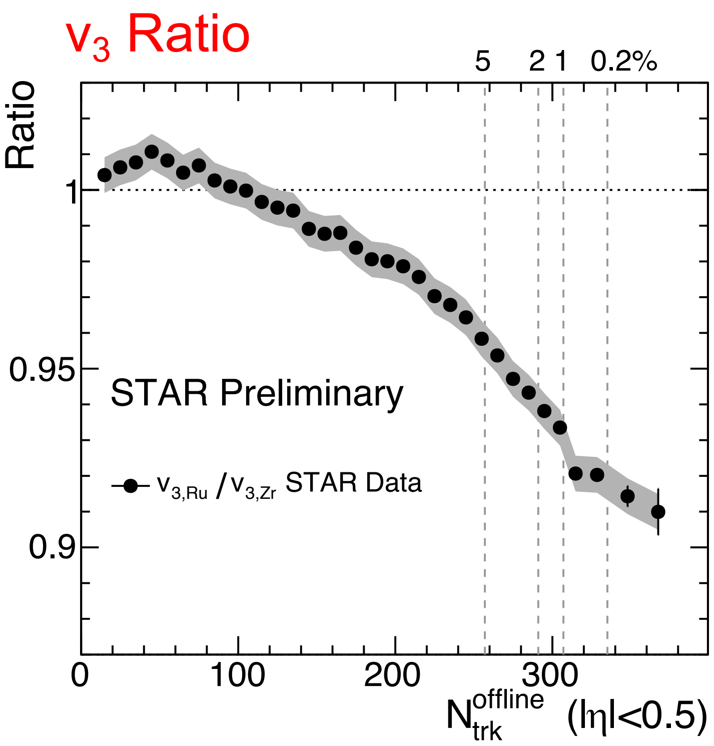

Nuclear structure via ^{96}Ru/^{96}Zr v_n ratio

v_2 Ratio

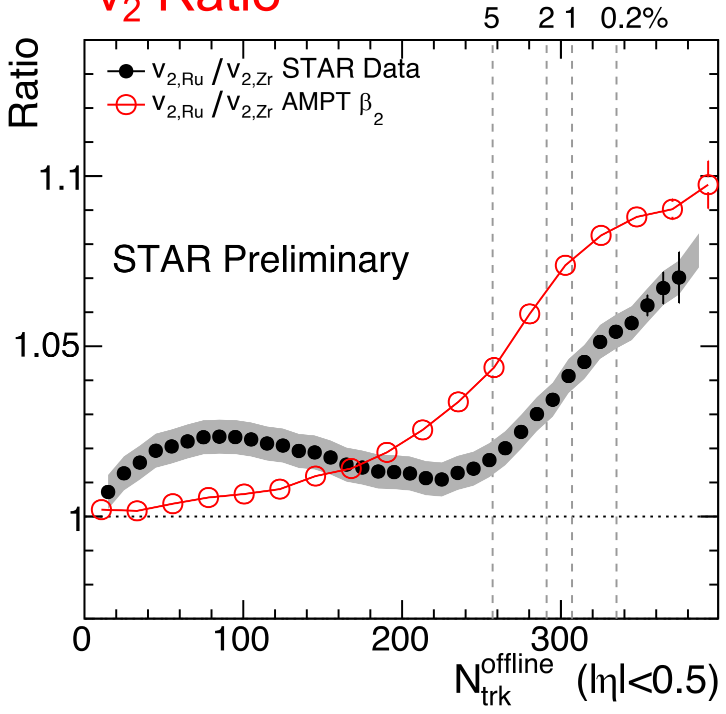

v_3 Ratio

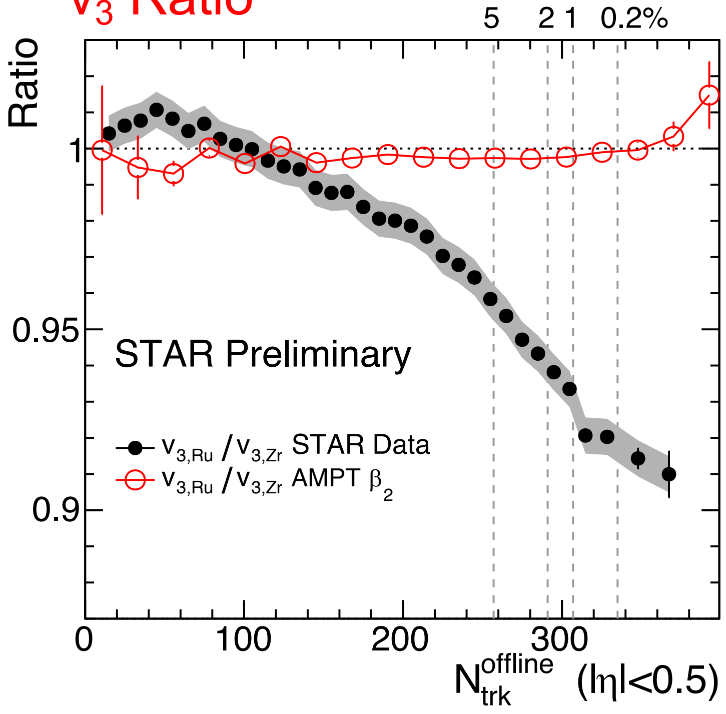

$\beta_{2,Ru}$ ~ 0.16 increase v_2, no influence on v_3 ratio

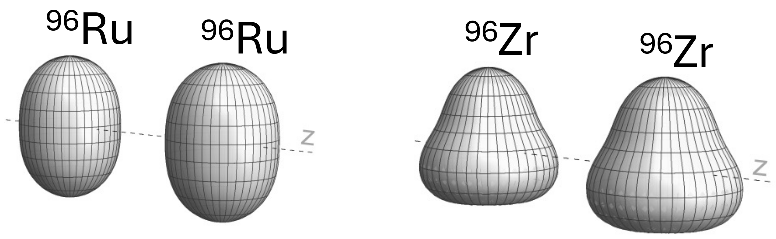

$$\beta_{2,\mathrm{Ru}} = 0.16 \pm 0.02$$

difference	$\Delta\beta_2^2$	$\Delta\beta_3^2$	Δa_0	ΔR_0
	0.0226	-0.04	-0.06 fm	0.07 fm

Current estimation is from transport model

Nuclear structure via ^{96}Ru/^{96}Zr v_n ratio

v_2 Ratio

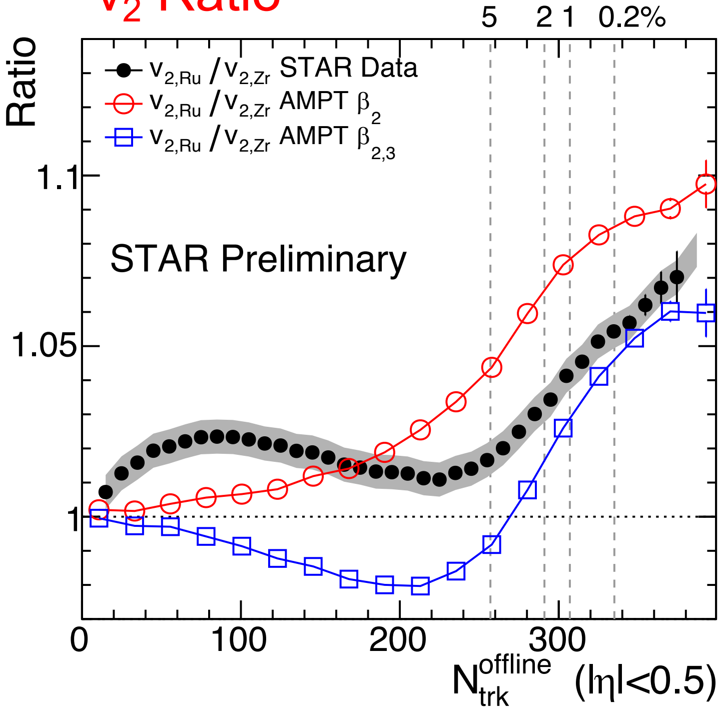

v_3 Ratio

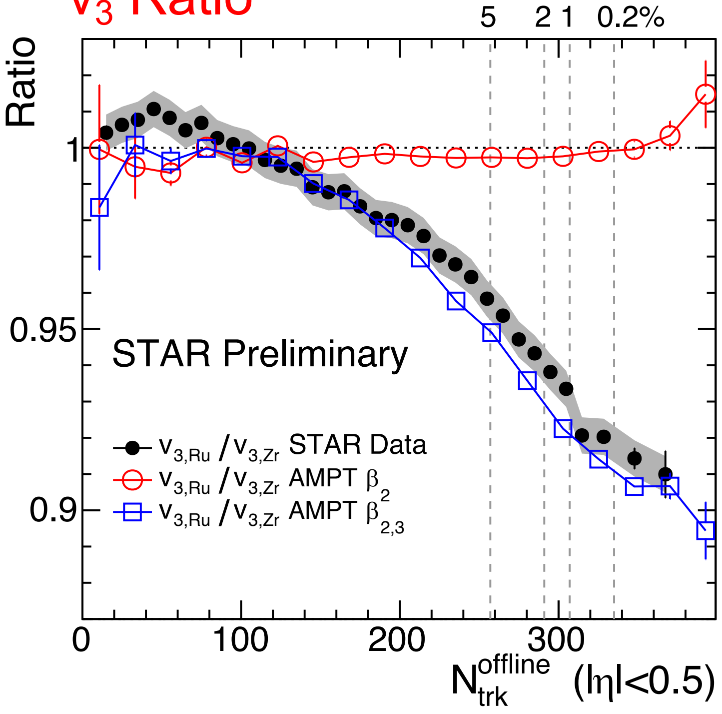

$\beta_{2,Ru} \sim 0.16$ increase v_2, no influence on v_3 ratio

$\beta_{3,Zr} \sim 0.2$ decrease v_2 in mid-central, decrease v_3 ratio

- Direct observation of octupole deformation in ^{96}Zr nucleus

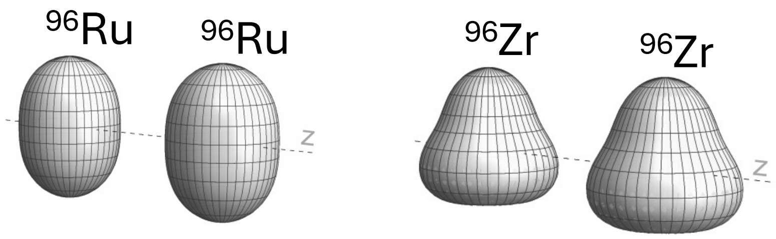

$\beta_{2,\mathrm{Ru}} = 0.16 \pm 0.02$ $\beta_{3,\mathrm{Zr}} = 0.20 \pm 0.02$

difference	$\Delta\beta_2^2$	$\Delta\beta_3^2$	Δa_0	ΔR_0
	0.0226	-0.04	-0.06 fm	0.07 fm

Current estimation is from transport model

Nuclear structure via ^{96}Ru/^{96}Zr v_n ratio

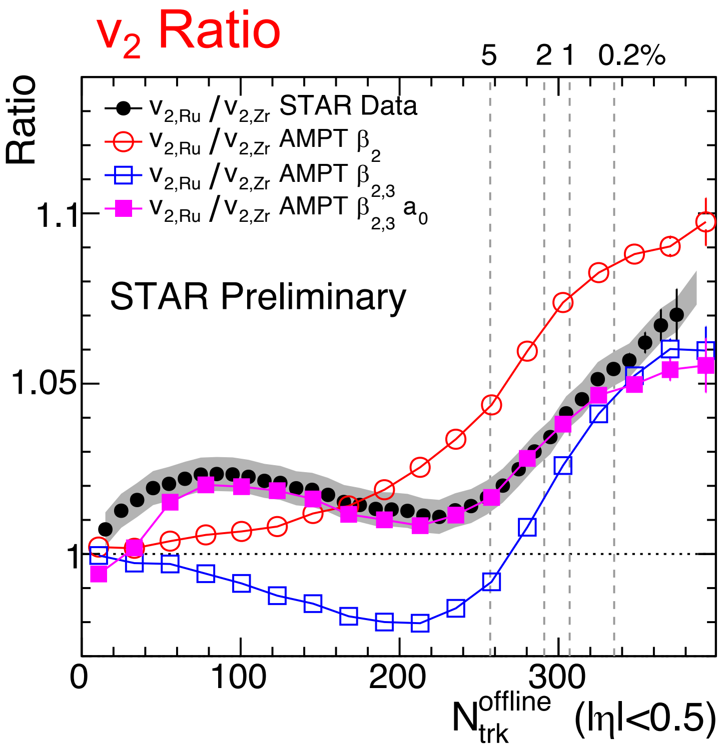

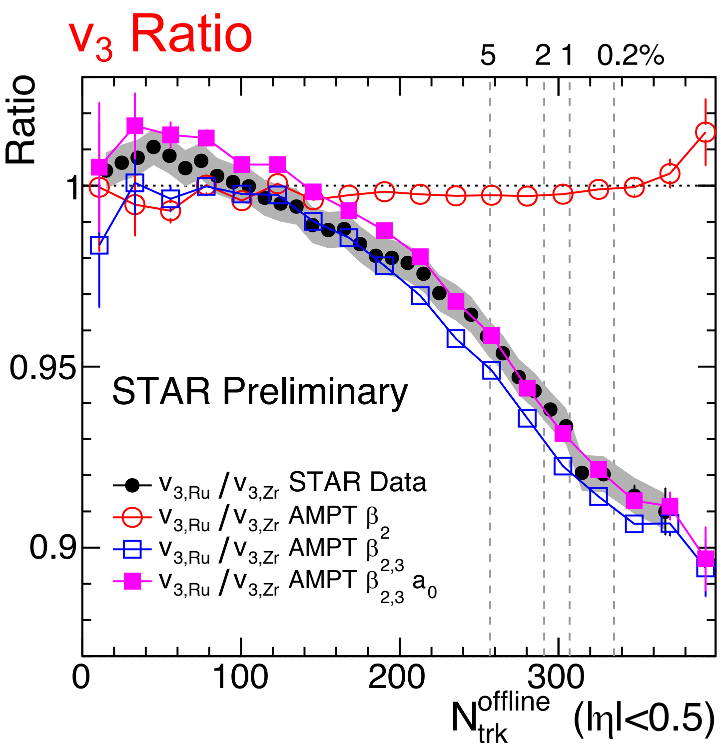

$\beta_{2,Ru} \sim 0.16$ increase v_2, no influence on v_3 ratio

$\beta_{3,Zr} \sim 0.2$ decrease v_2 in mid-central, decrease v_3 ratio

$\Delta a_0 = -0.06$ fm increase v_2 mid-central, small impact on v_3

- Direct observation of octupole deformation in ^{96}Zr nucleus
- Imply the neutron skin difference between ^{96}Ru and ^{96}Zr

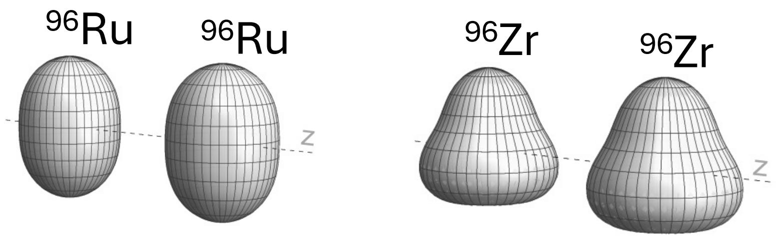

$\beta_{2,\mathrm{Ru}} = 0.16 \pm 0.02$ $\beta_{3,\mathrm{Zr}} = 0.20 \pm 0.02$

difference	$\Delta\beta_2^2$	$\Delta\beta_3^2$	Δa_0	ΔR_0
	0.0226	-0.04	-0.06 fm	0.07 fm

Current estimation is from transport model

Nuclear structure via $^{96}Ru/^{96}Zr$ v_n ratio

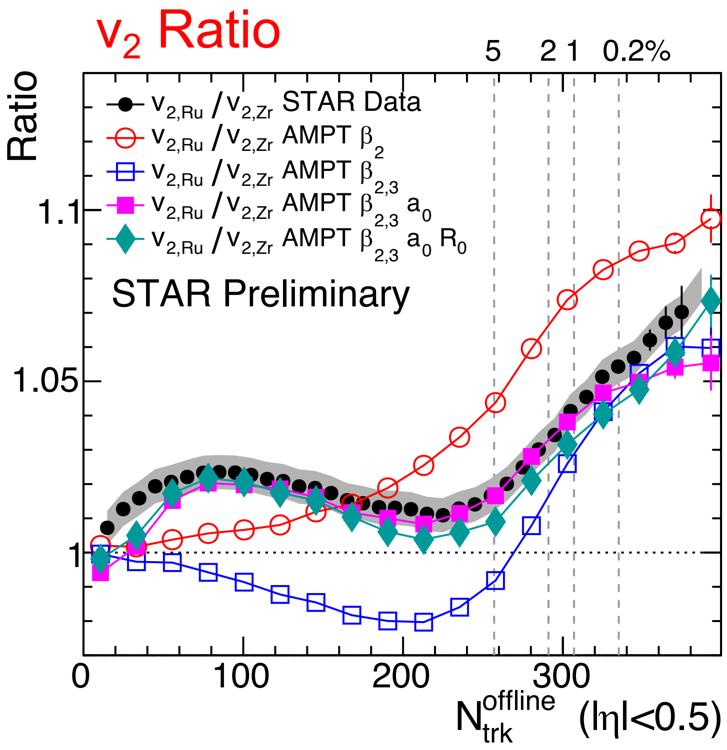

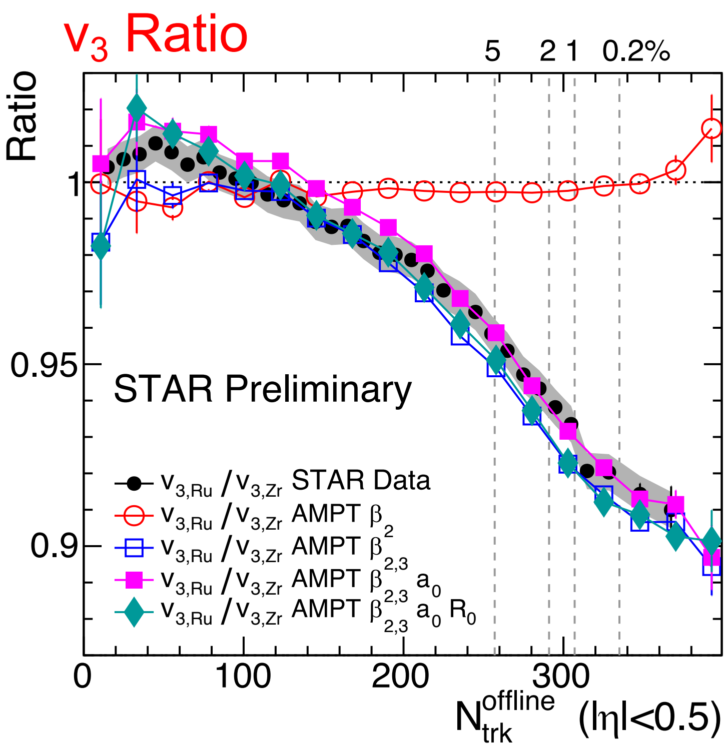

$\beta_{2,Ru}$ ~ 0.16 increase v_2, no influence on v_3 ratio

$\beta_{3,Zr}$ ~ 0.2 decrease v_2 in mid-central, decrease v_3 ratio

Δa_0 = -0.06 fm increase v_2 mid-central, small impact on v_3

Radius ΔR_0 = 0.07 fm only slightly affects v_2 and v_3 ratio.

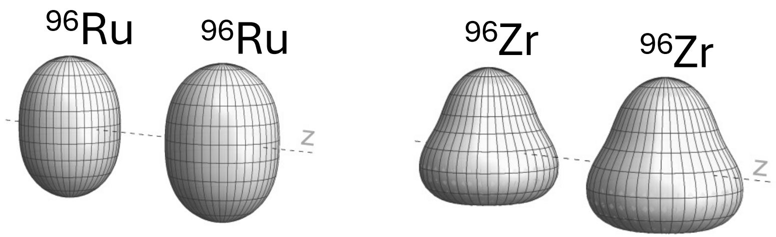

- Direct observation of octupole deformation in ^{96}Zr nucleus
- Imply the neutron skin difference between ^{96}Ru and ^{96}Zr
- Simultaneously constrain parameters using Bayesian analysis

$$R_{\mathcal{O}} \equiv \frac{\mathcal{O}_{\rm Ru}}{\mathcal{O}_{\rm Zr}} \approx 1 + c_1\Delta\beta_2^2 + c_2\Delta\beta_3^2 + c_3\Delta R_0 + c_4\Delta a$$

$\beta_{2,\rm Ru} = 0.16 \pm 0.02$ $\quad$ $\beta_{3,\rm Zr} = 0.20 \pm 0.02$

difference	$\Delta\beta_2^2$	$\Delta\beta_3^2$	Δa_0	ΔR_0
	0.0226	-0.04	-0.06 fm	0.07 fm

Current estimation is from transport model

C. Zhang and J. Jia, PRL128, 022301(2022); J. Jia, C. Zhang, PRC 107, L012901(2023)

Light nuclear geometry and nucleon nucleon correlations

Nucleon fluctuation

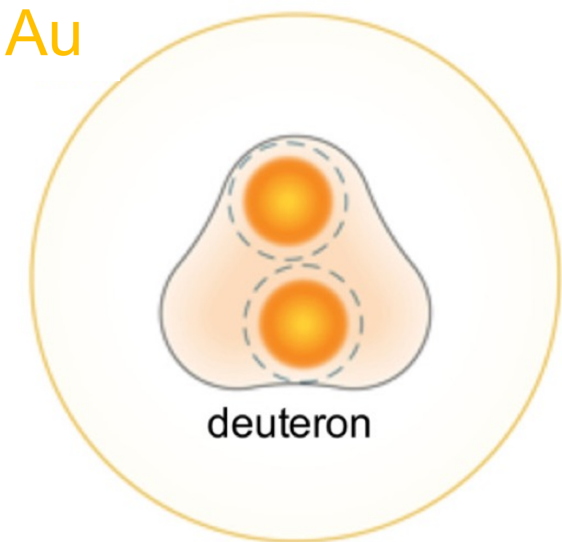

Nucleon & subnucleon fluctuation

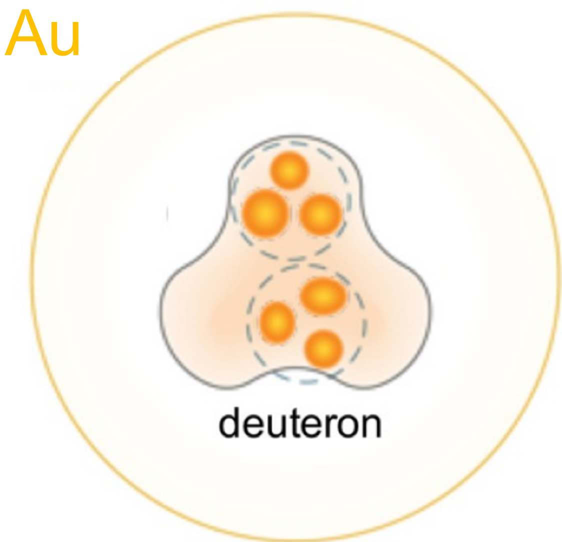

Nucleon-nucleon correlation

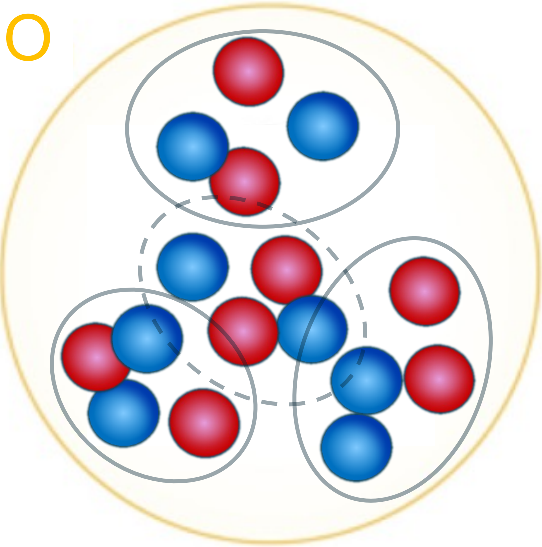

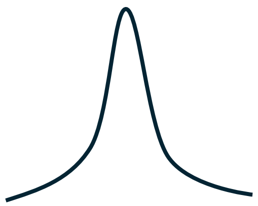

$p(\alpha)$

ab initio calculations

STAR, PRL 130, 242301 (2023)

STAR, PRC 110, 064902 (2024)

W. He, Y. Ma et al., PRL 113, 032506 (2014);…

C. Zhang, J. Chen, G. Giacalone, S. Huang, J. Jia, Y. Ma, PLB 862, 139322 (2025)

S. Huang, J. Jia, C. Zhang, 2507.16162

…

d+Au collision, 200 GeV ⟷ Nearly same N_{ch} ⟷ O+O collision, 200 GeV

Benchmarking geometric tomography of ^{16}O nucleus

New

STAR paper is in Collaboration Review

More details in Jiangyong's talk

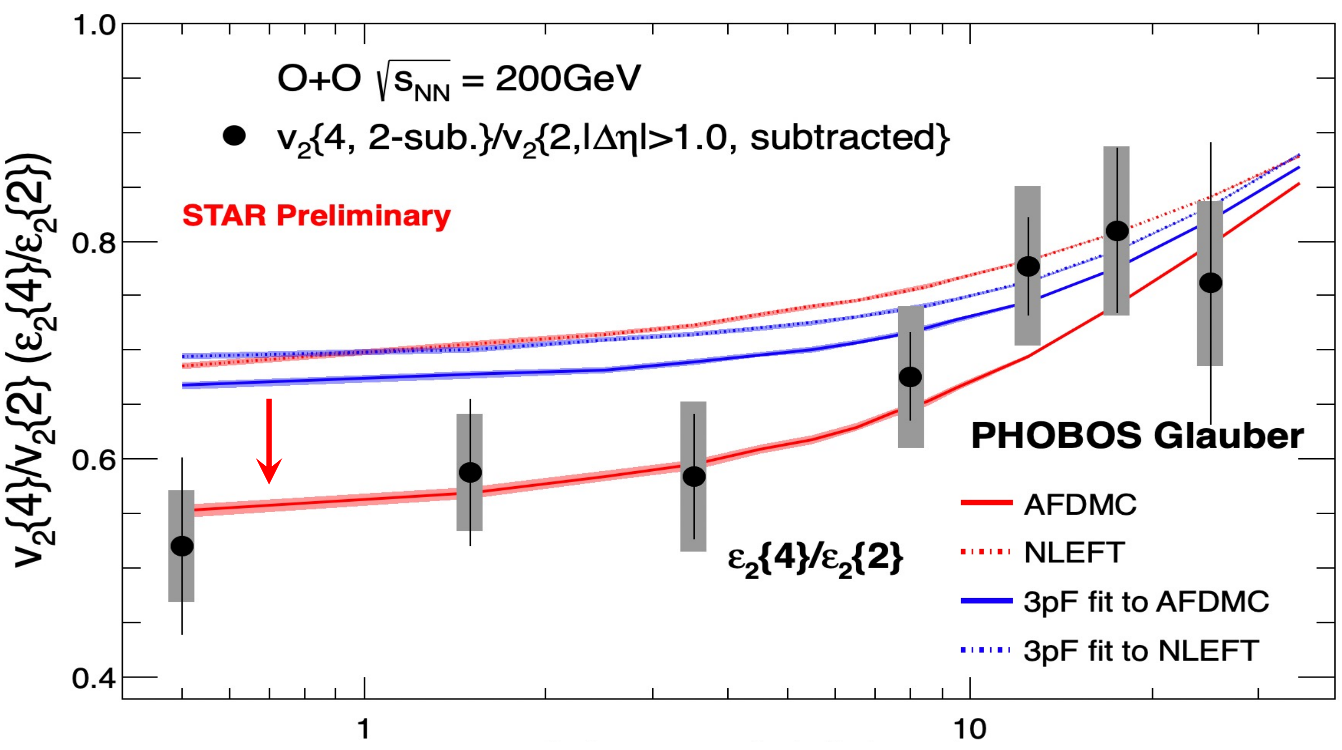

$$(v_n\{2\})^2 = c_n\{2\} = \langle v_n^2 \rangle$$
$$(v_n\{4\})^4 = -c_n\{4\} = 2\langle v_n^2 \rangle^2 - \langle v_n^4 \rangle$$

$$\varepsilon_2\{2\}^2 = \langle \varepsilon_2^2 \rangle$$
$$\varepsilon_2\{4\}^4 = 2\langle \varepsilon_2^2 \rangle^2 - \langle \varepsilon_2^4 \rangle$$

$\varepsilon_2\{4\}$ /$\varepsilon_2\{2\}$ from three models:

1. WS is away from STAR data.

2. VMC and EFT have a visible difference.

Can many-nucleon correlations significantly impact the eccentricity fluctuations? YES!

VMC and EFT theory have visible differences describing the $v_2\{4\}/v_2\{2\}$. The interplay between sub-nucleon fluctuation and many-nucleon correlation.

STAR, PRL 130, 242301 (2023)

Y. Ma, S. Zhang, Handbook of Nuclear Physics (2022); W. He, Y. Ma et al, PRL 113, 032506 (2014)

G. Giacalone, G. Nijs et al., PRL135, 012302 (2025), G. Giacalone, W. Zhao et al., PRL134, 082301 (2025); *C. Zhang, J. Chen, G. Giacalone, S. Huang, J. Jia, Y. Ma, PLB 862, 139322 (2025)*

Y. Wang, S. Zhao, B. Cao, H. Xu, H. Song, PRC 109, L051904 (2024); X. Zhao, G. Ma. Y. Zhou, Z. Lin, C. Zhang, 2404.09780; S. Jahan, Roch, C. Shen, 2507. 11394

Benchmarking geometric tomography of ^{16}O nucleus

New

STAR paper is in Collaboration Review

More details in Jiangyong's talk

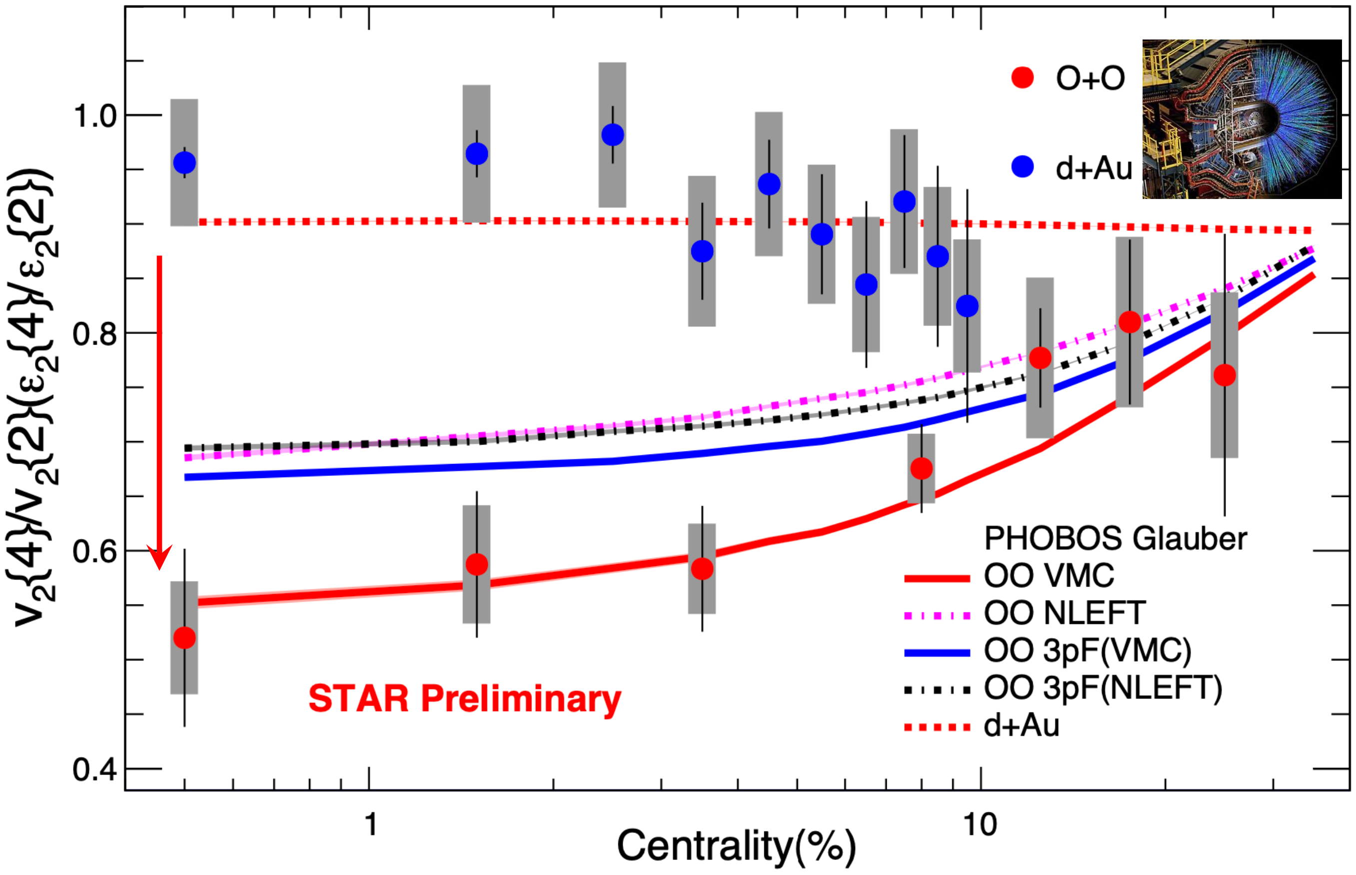

$$(v_n\{2\})^2 = c_n\{2\} = \langle v_n^2 \rangle \qquad \varepsilon_2\{2\}^2 = \langle \varepsilon_2^2 \rangle$$

$$(v_n\{4\})^4 = -c_n\{4\} = 2\langle v_n^2 \rangle^2 - \langle v_n^4 \rangle \qquad \varepsilon_2\{4\}^4 = 2\langle \varepsilon_2^2 \rangle^2 - \langle \varepsilon_2^4 \rangle$$

$\varepsilon_2\{4\}/\varepsilon_2\{2\}$ from three models:

1. WS is away from STAR data.

2. VMC and EFT have a visible difference.

Can many-nucleon correlations significantly impact the eccentricity fluctuations? YES!

VMC and EFT theory have visible differences describing the $v_2\{4\}/v_2\{2\}$. The interplay between sub-nucleon fluctuation and many-nucleon correlation.

STAR, PRL 130, 242301 (2023)

Geometric scan elucidates nuclear tomography and strong nuclear force?

Need more low-energy model inputs.

Y. Ma, S. Zhang, Handbook of Nuclear Physics (2022); W. He, Y. Ma et al, PRL 113, 032506 (2014)

G. Giacalone, G. Nijs et al., PRL135, 012302 (2025), G. Giacalone, W. Zhao et al., PRL134, 082301 (2025); *C. Zhang, J. Chen, G. Giacalone, S. Huang, J. Jia, Y. Ma, PLB 862, 139322 (2025)*

Y. Wang, S. Zhao, B. Cao, H. Xu, H. Song, PRC 109, L051904 (2024); X. Zhao, G. Ma. Y. Zhou, Z. Lin, C. Zhang, 2404.09780; S. Jahan, Roch, C. Shen, 2507. 11394

Benchmarking geometric tomography of ^{16}O nucleus

New

STAR paper is in Collaboration Review

More details in Jiangyong's talk

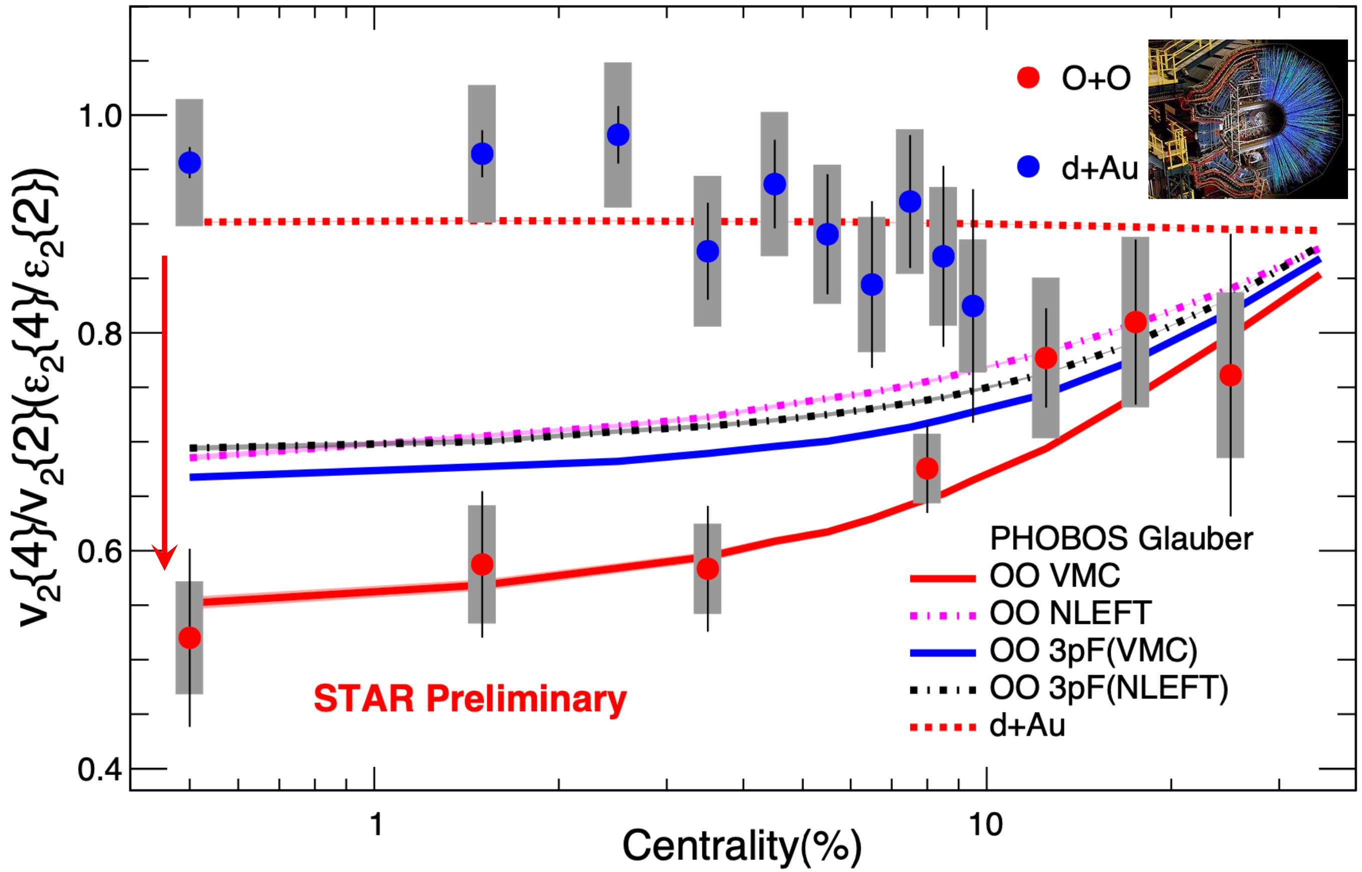

$$(v_n\{2\})^2 = c_n\{2\} = \langle v_n^2 \rangle \qquad \varepsilon_2\{2\}^2 = \langle \varepsilon_2^2 \rangle$$

$$(v_n\{4\})^4 = -c_n\{4\} = 2\langle v_n^2 \rangle^2 - \langle v_n^4 \rangle \qquad \varepsilon_2\{4\}^4 = 2\langle \varepsilon_2^2 \rangle^2 - \langle \varepsilon_2^4 \rangle$$

$\varepsilon_2\{4\}/\varepsilon_2\{2\}$ from three models:

1. WS is away from STAR data.

2. VMC and EFT have a visible difference.

Can many-nucleon correlations significantly impact the eccentricity fluctuations? YES!

VMC and EFT theory have visible differences describing the $v_2\{4\}/v_2\{2\}$. The interplay between sub-nucleon fluctuation and many-nucleon correlation.

STAR, PRL 130, 242301 (2023)

Geometric scan elucidates nuclear tomography and strong nuclear force?

Need more low-energy model inputs.

LHC (ALICE, ATLAS, CMS, LHCb) released the O+O/Ne+Ne!!!
Shape imaging method for light ions (New avenue)

Y. Ma, S. Zhang, Handbook of Nuclear Physics (2022); W. He, Y. Ma et al, PRL 113, 032506 (2014)

G. Giacalone, G. Nijs et al., PRL135, 012302 (2025), G. Giacalone, W. Zhao et al., PRL134, 082301 (2025); *C. Zhang, J. Chen, G. Giacalone, S. Huang, J. Jia, Y. Ma, PLB 862, 139322 (2025)*

Y. Wang, S. Zhao, B. Cao, H. Xu, H. Song, PRC 109, L051904 (2024); X. Zhao, G. Ma. Y. Zhou, Z. Lin, C. Zhang, 2404.09780; S. Jahan, Roch, C. Shen, 2507. 11394

New radial flow $v_0(p_T)$ measurement in 200 GeV

Radial expansion: the n=0 modulation

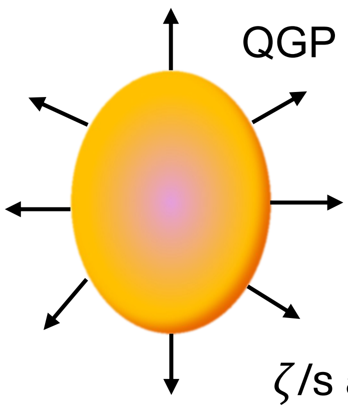

J. Jia, 2507.14399

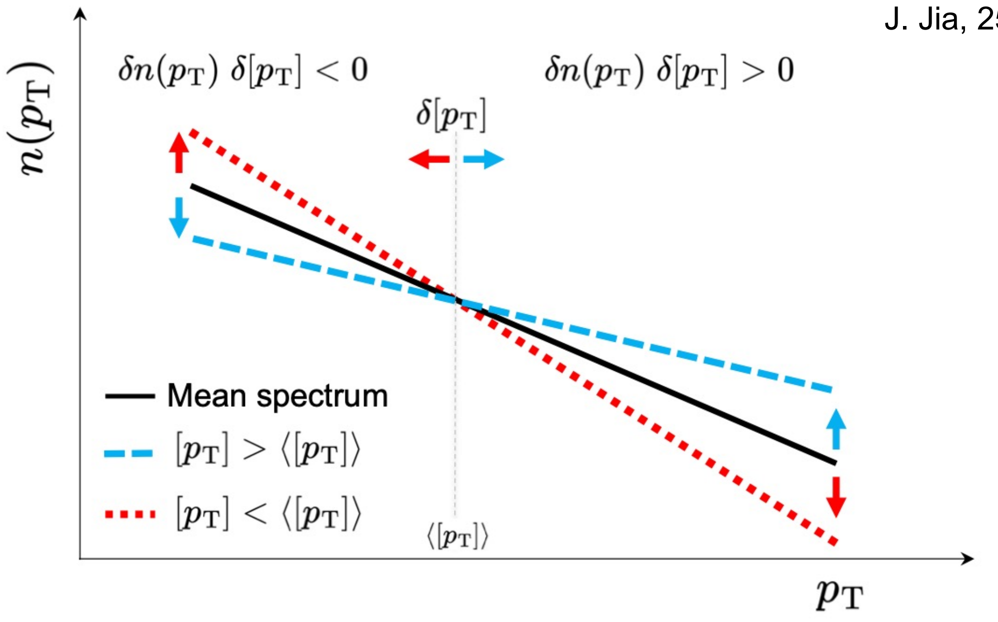

Spectra slope quantified by $[p_T]$ in each event:
Fluctuation in $[p_T]$ →Fluctuation in spectra.

Quantify the correlation induced by radial flow using **covariance between $n(p_T)$ and $[p_T]$:** $\langle \delta n\,(p_T)\delta\,[p_T] \rangle$

Calculated within a reference range, p_T-independent.

$$v_0\,(p_T) = \frac{\langle \delta n\,(p_T)\delta\,[p_T] \rangle}{\langle n\,(p_T) \rangle\,\langle [p_T] \rangle} \times \frac{1}{v_{0,\mathrm{int}}}$$

$$v_{0,\,\mathrm{int}} \equiv \frac{\sqrt{\langle (\delta\,[p_T])^2 \rangle}}{\langle [p_T] \rangle}$$

Pearson Correlations between local possiblity of particle yield and reference mean p_T from spectra

Remove influence from global fluctuations

B. Schenke, C. Shen, D. Teaney, PRC 102, 034905 (2020)
T. Parida, R. Samanta, J.Y. Ollitrault, PLB 857, 138985 (2024)
S. A. Jahan, H. Roch, C. Shen. arXiv: 2507.11394
L. Du, 2508.07184

This allows us to verify the signatures of collectivity for radial flow, like for anisotropic flow

Radial flow $v_0(p_T)$ in system-size comparison

New

First measurement at RHIC --- Zaining Wang (Fudan & Stony Brook), IS 2025

Au+ Au vs. O+O

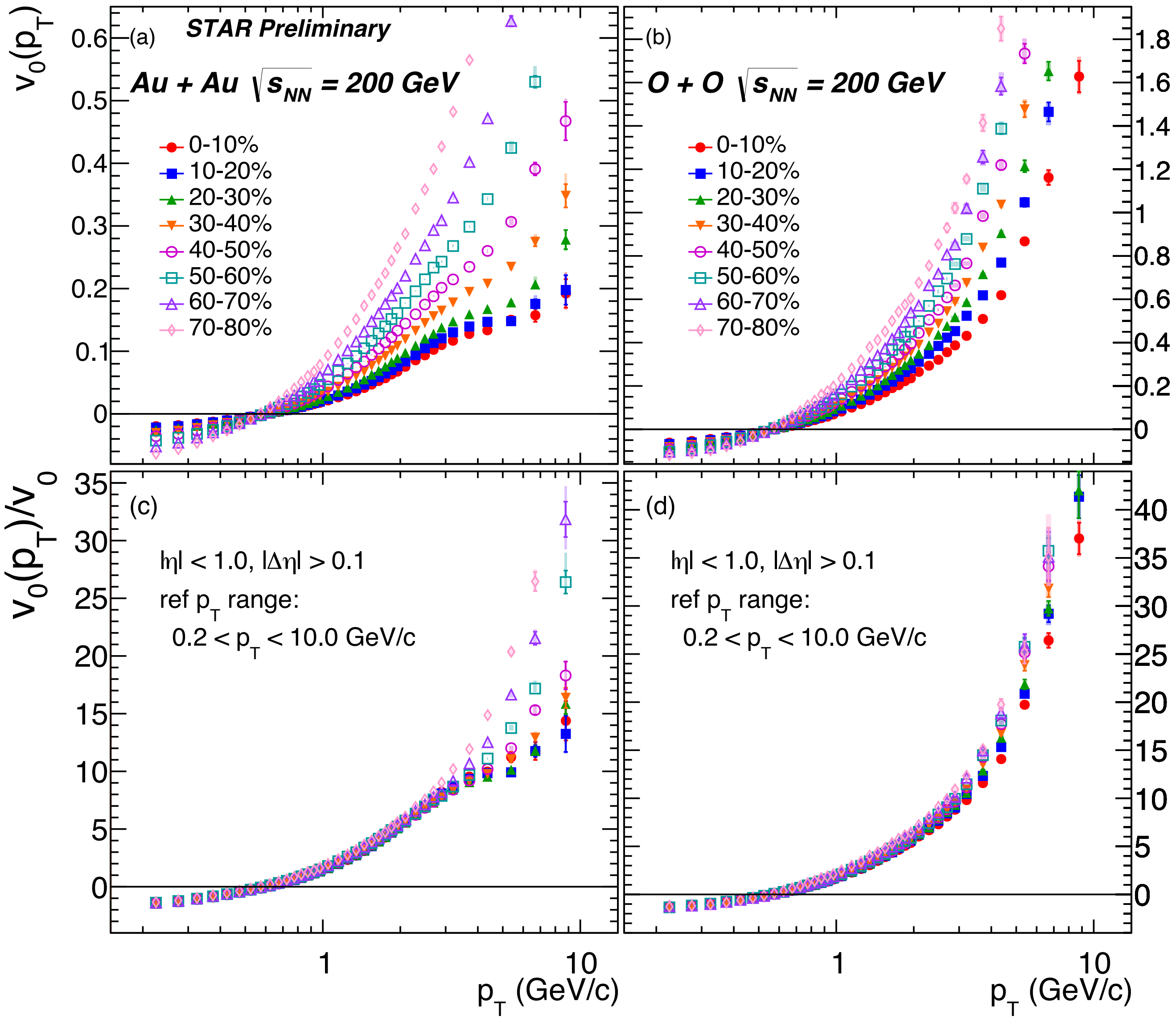

Increase with p_T
Exhibiting a strong centrality dependence.
The zero-crossing point coincides with $\langle [p_T] \rangle$, where fluctuations vanish

After normalization, all centralities collapse onto a single trend, indicating a hydrodynamic collective response to global fluctuations

$$v_0(p_T) = \frac{\langle \delta n(p_T)\, \delta [p_T]_{p_T^{ref}} \rangle}{\langle \delta n(p_T) \rangle \left(\langle \delta [p_T] \rangle v_0 \right)_{p_T^{ref}}}$$

Bulk viscosity sensitivity

New

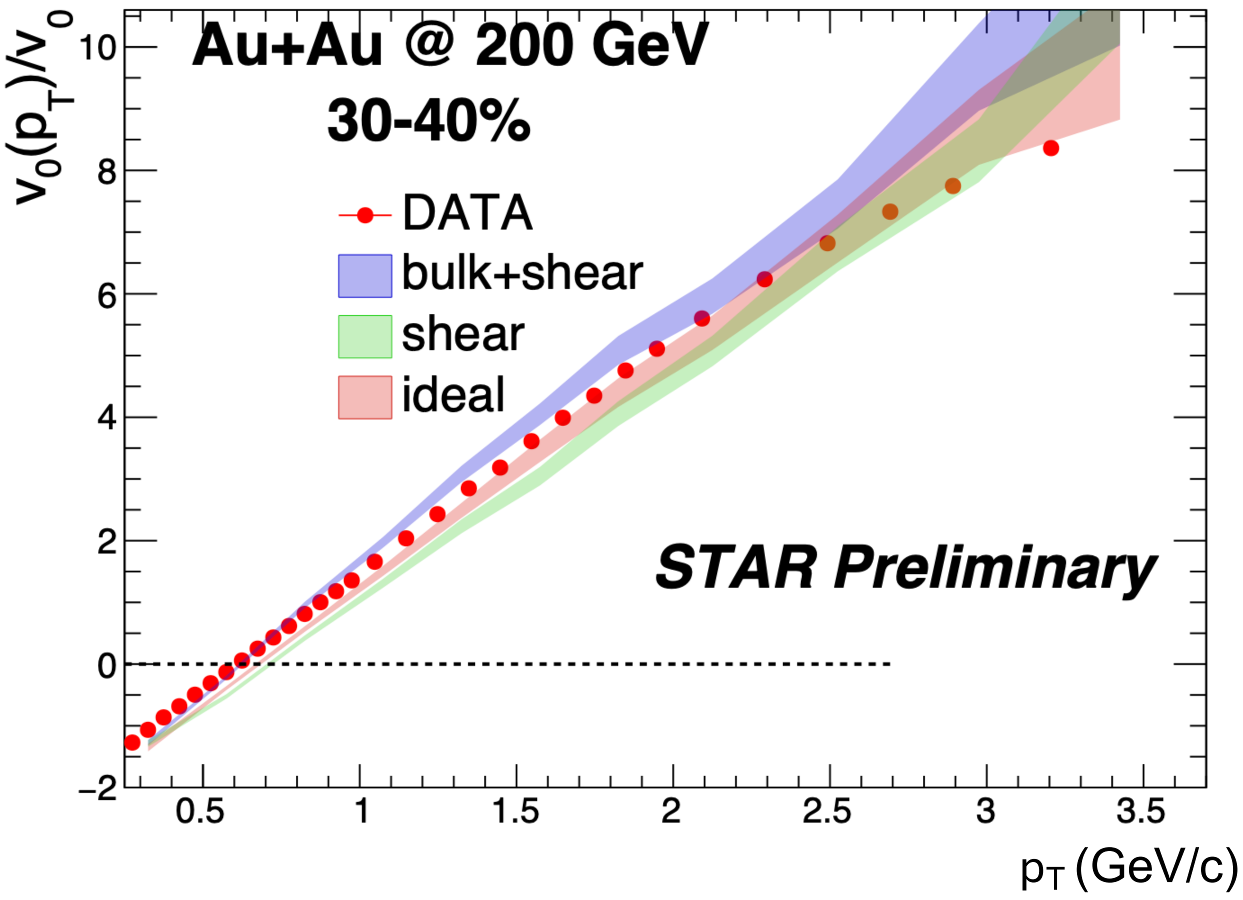

It demonstrated to have a strong bulk viscosity

Only a weak dependence on shear viscosity, which is suggested by comparison in models (need to check more)

Model calculations are from Lipei Du

PID measurement and data-model comparisons

New

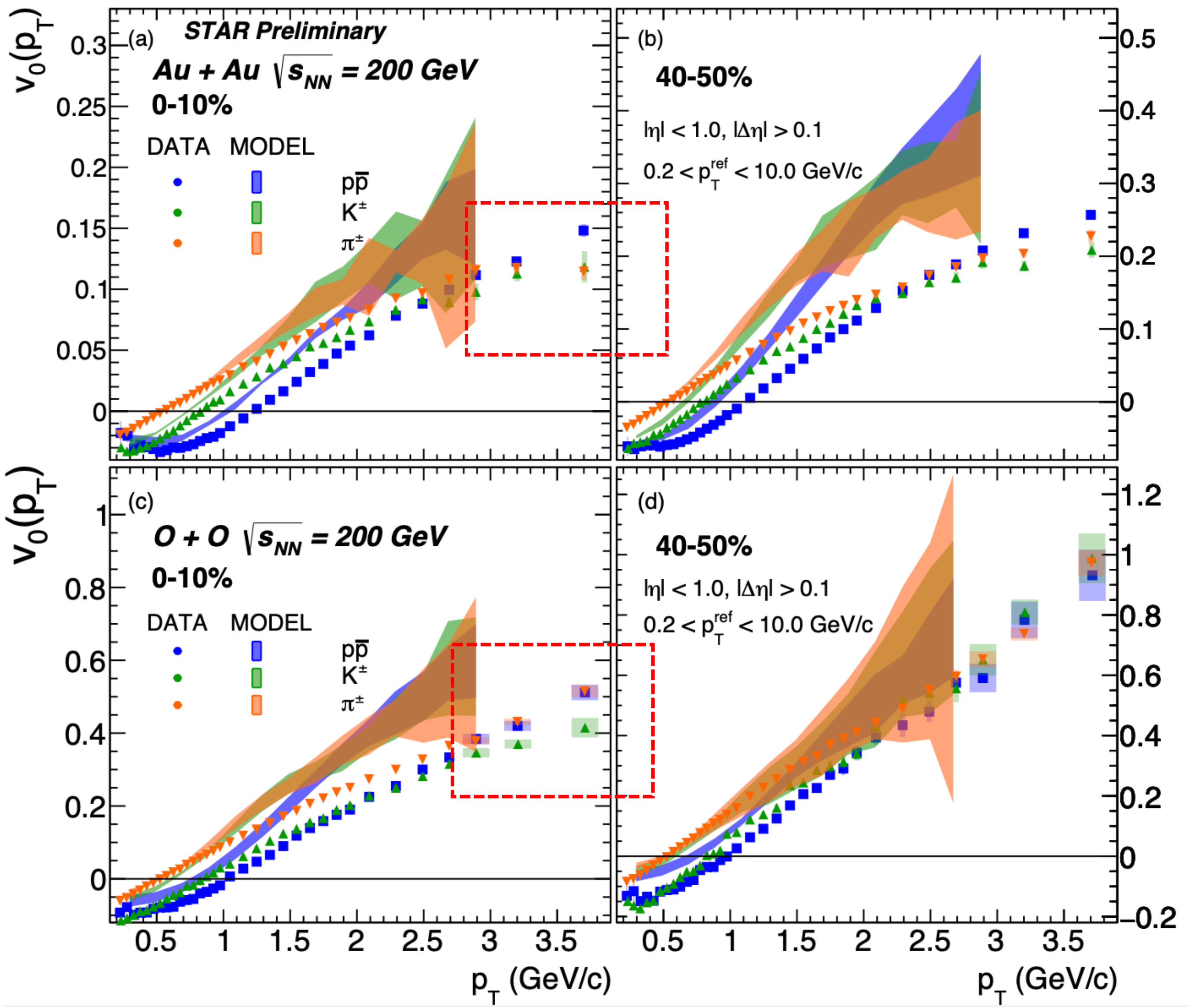

$$v_0(p_T) = \frac{\langle \delta n(p_T)\, \delta[p_T]_{p_T^{ref}} \rangle}{\langle \delta n(p_T) \rangle \left(\langle \delta[p_T] \rangle v_0 \right)_{p_T^{ref}}}$$

The stronger boost experienced by heavier particles gives rise to a clear mass ordering

Meson-baryon splitting are observed

3D-Glauber+MUSIC+UrQMD model also show clear mass ordering, but seems deviate from data

Model calculations are from Chun Shen

PID measurement and data-model comparisons

New

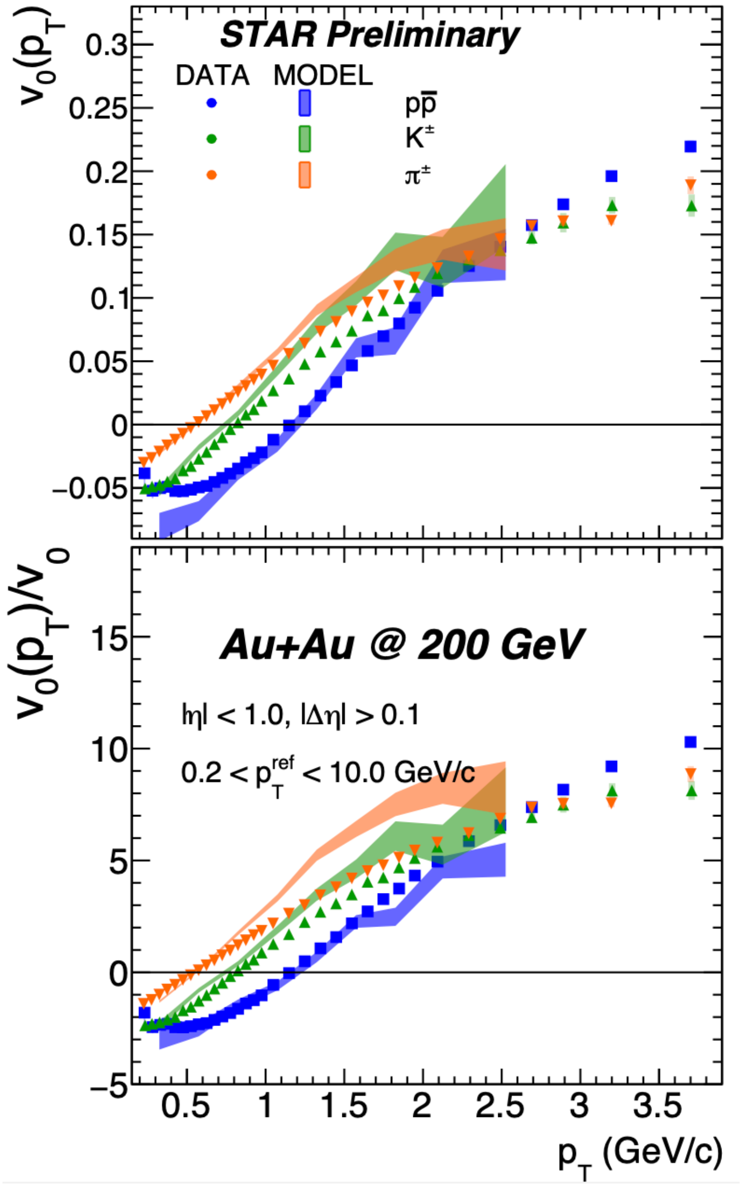

$$v_0(p_T) = \frac{\langle \delta n(p_T)\, \delta[p_T]_{p_T^{ref}} \rangle}{\langle \delta n(p_T) \rangle \, (\langle \delta [p_T] \rangle v_0)_{p_T^{ref}}}$$

TRENTo+free-streaming+MUSIC+iSS+SMASH show good comparison

More model calculations are needed to tune for fitting this new observables at RHIC energies.

Model calculations are from Lipei Du

Energy evolution from LHC to RHIC energies

New

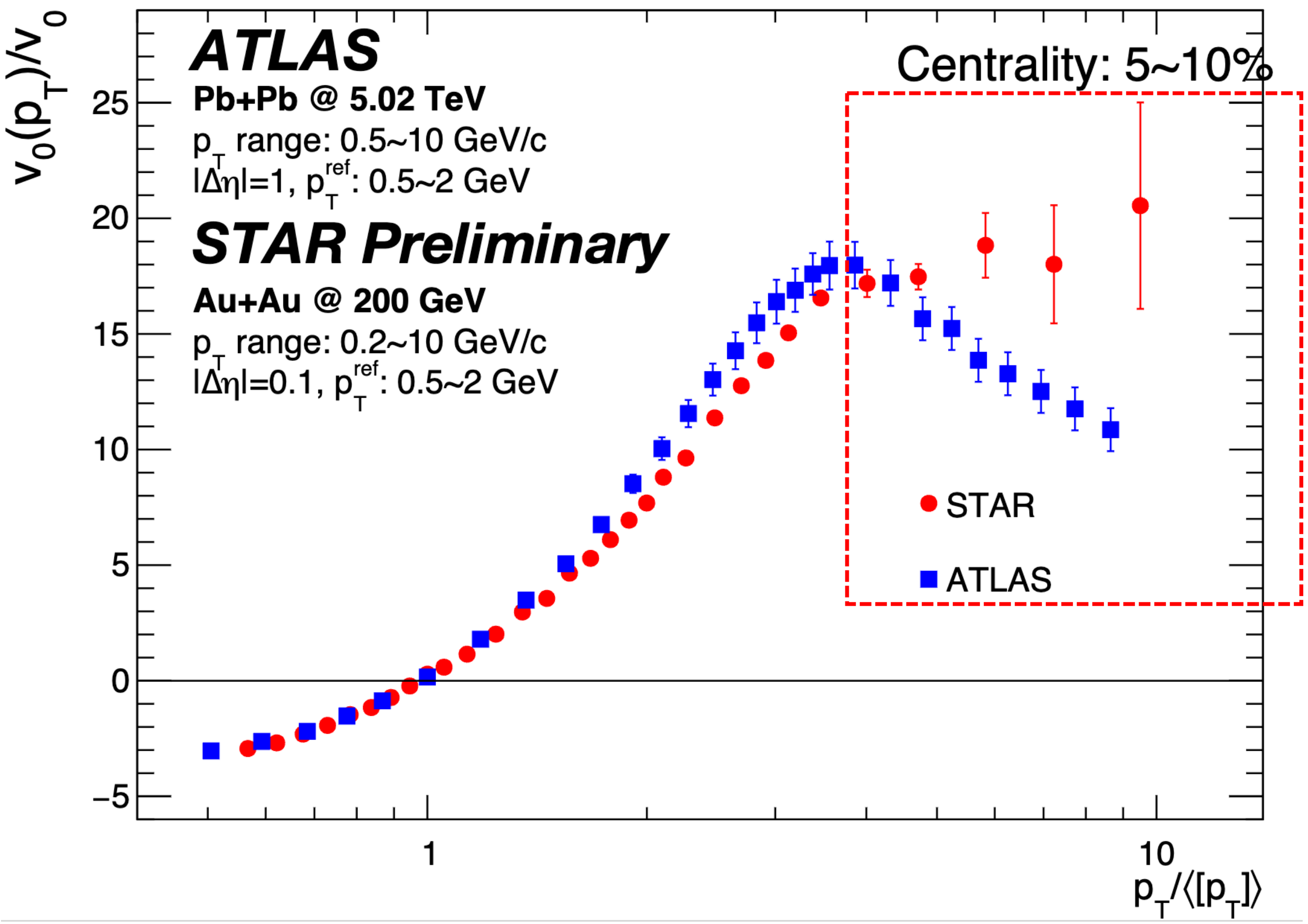

Close radial expansion between the LHC and RHIC measurements with similar slope at low p_T

$p_T > 4$ GeV/c region is different, different jet quenching effect?

1) Will add the ALICE, ATLAS, and STAR together. 2) Would also expect nuclear structure features in n=0 modulations? U+U/Au+Au, Ru+Ru/Zr+Zr, …

Future system- and energy-scans are interesting and useful for understanding radial flow

IV. Conclusions and Outlooks

1. The signatures of nuclear structure in nuclear collisions are ubiquitous:

STAR, Nature 635, 67-72 (2024); 2506.17785

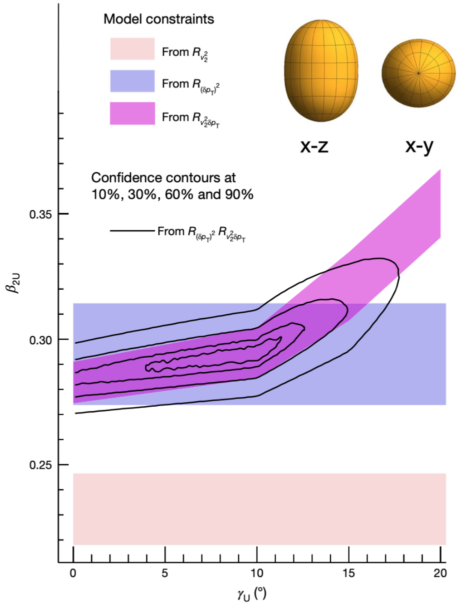

$\beta_{2U} = 0.286 \pm 0.025; \quad \gamma_U = 8.5^\circ \pm 4.8^\circ$

$\beta_{3U} = 0.08 - 0.1; \quad \beta_{3U} \sim \beta_{4U}$

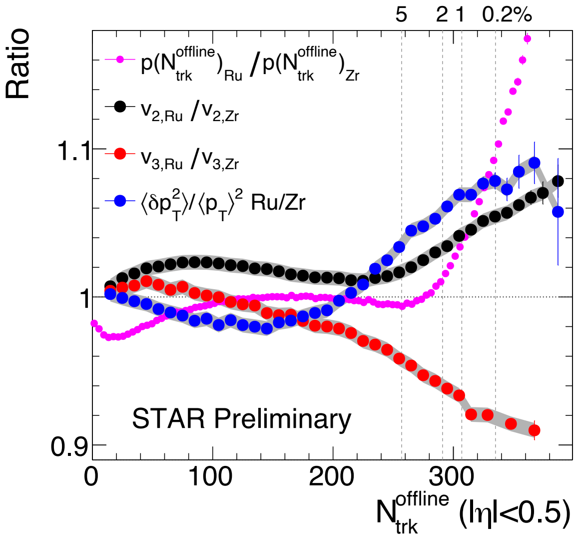

$\beta_{2,\text{Ru}} = 0.16 \pm 0.02; \quad \beta_{3,\text{Zr}} = 0.20 \pm 0.02$

	$\Delta\beta_2^2$	$\Delta\beta_3^2$	Δa_0	ΔR_0
difference	0.0226	-0.04	$-0.06\ fm$	$0.07\ fm$

STAR paper is in Collaboration Review

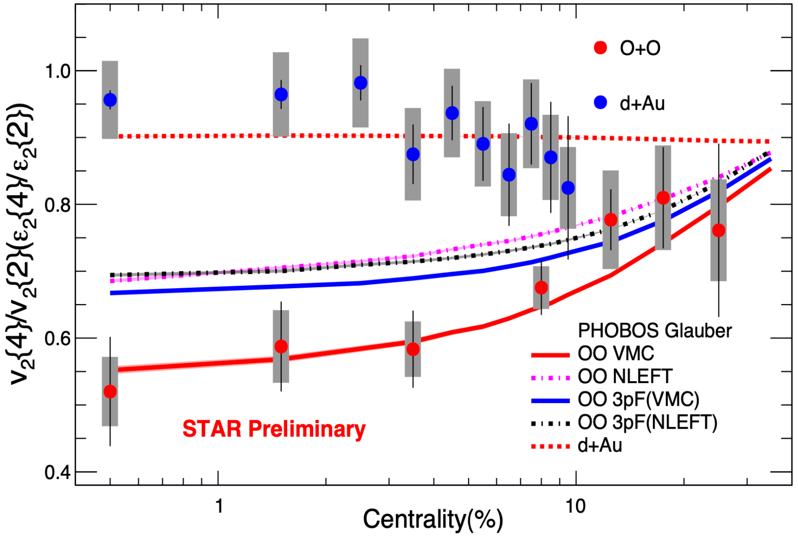

Nucleon-nucleon correlation is remarkable

Nuclear mass number (A)

2. Many potential applications from large to small collision systems :

→ Nucleosynthesis, nuclear fission, $0\nu\beta\beta$

→ Rigid and soft β_n and γ (shape fluctuations/coexistence)

→ Neutron skin

→ Energy evolution between GeV/TeV and MeV in even-and odd-A nuclei

IV. Conclusions and Outlooks

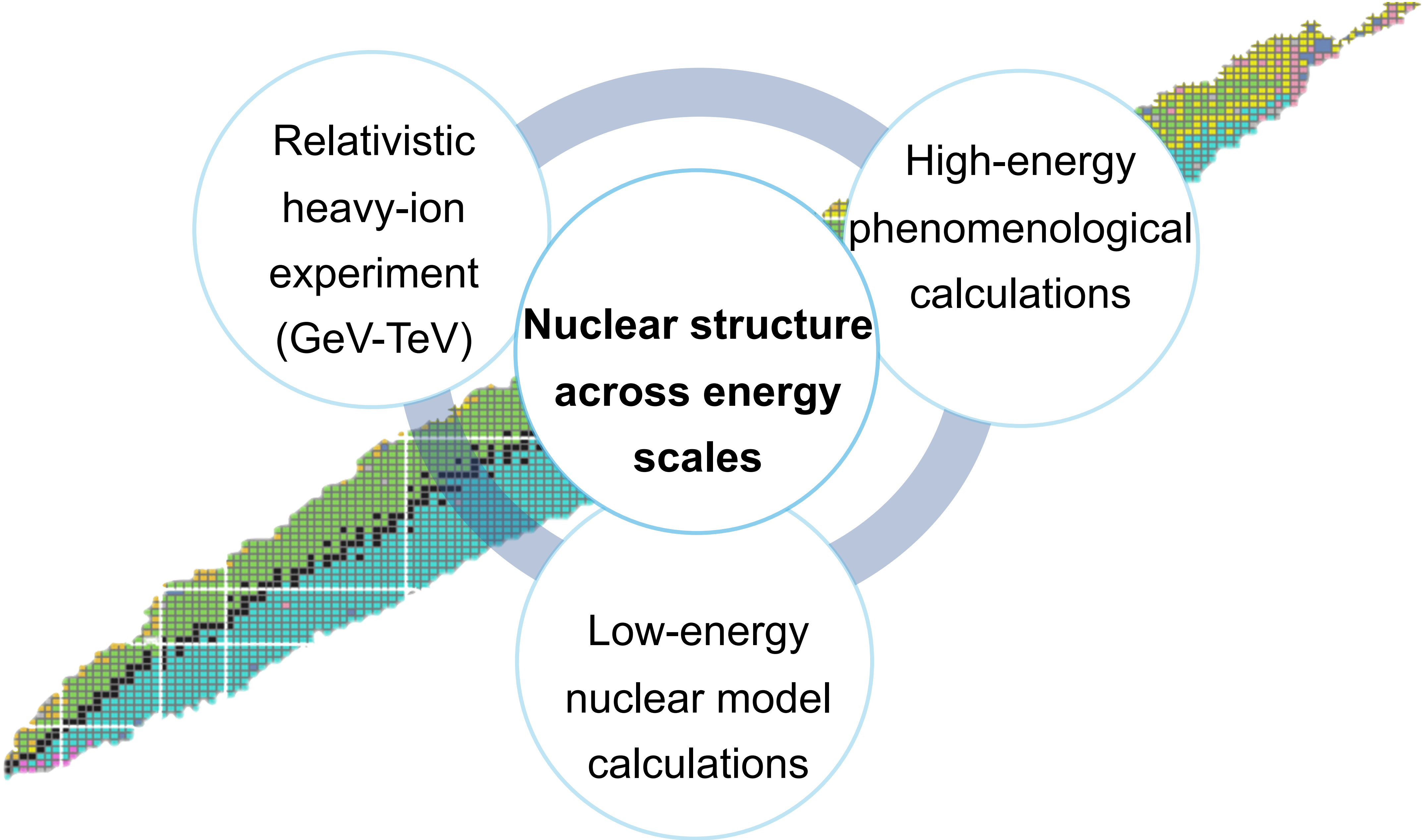

$[p_T]$ fluctuations as other novel tool

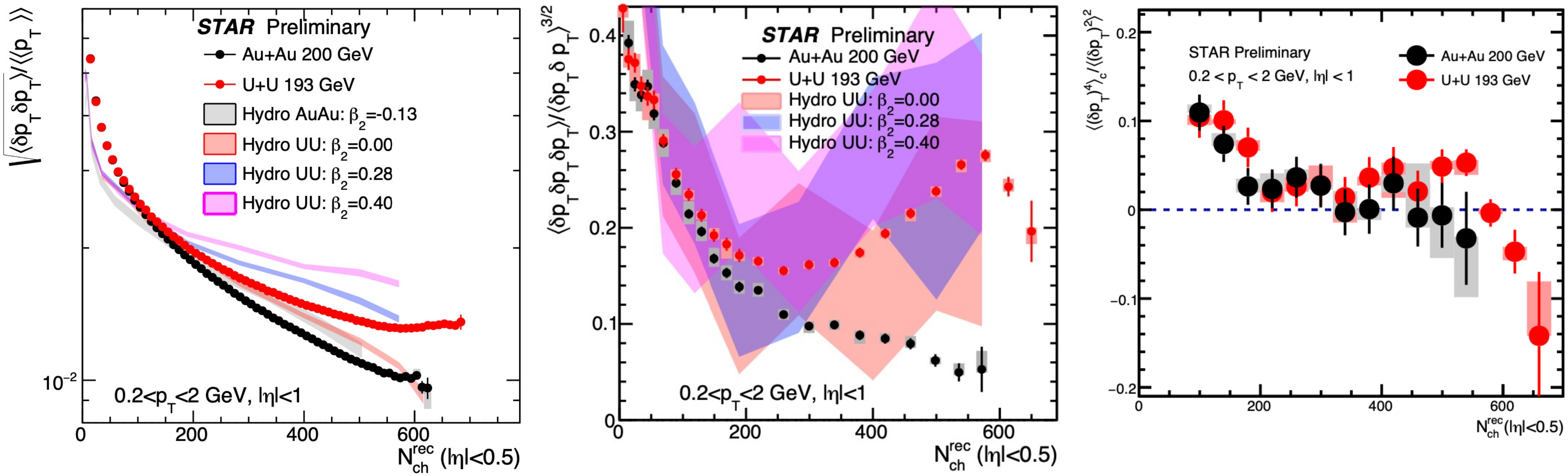

Au+Au: variance and skewness follow independent source scaling $1/N_s^{n-1}$ within power-law decrease

U+U: large enhancement in normalized variance and skewness and sign-change in normalized kurtosis
⟶ size fluctuations enhanced

The nuclear deformation role is further confirmed by hydro calculations. But we need more statistics.

$[p_T]$ fluctuations also serve as a good observable to explore the role of nuclear deformation.

ALICE, PLB 850, 138541 (2024); ATLAS, PRL 133, 252301 (2024)

Viscosity, nuclear parameters, and model variations

1) Taking the ratios cancels the viscosity effects.

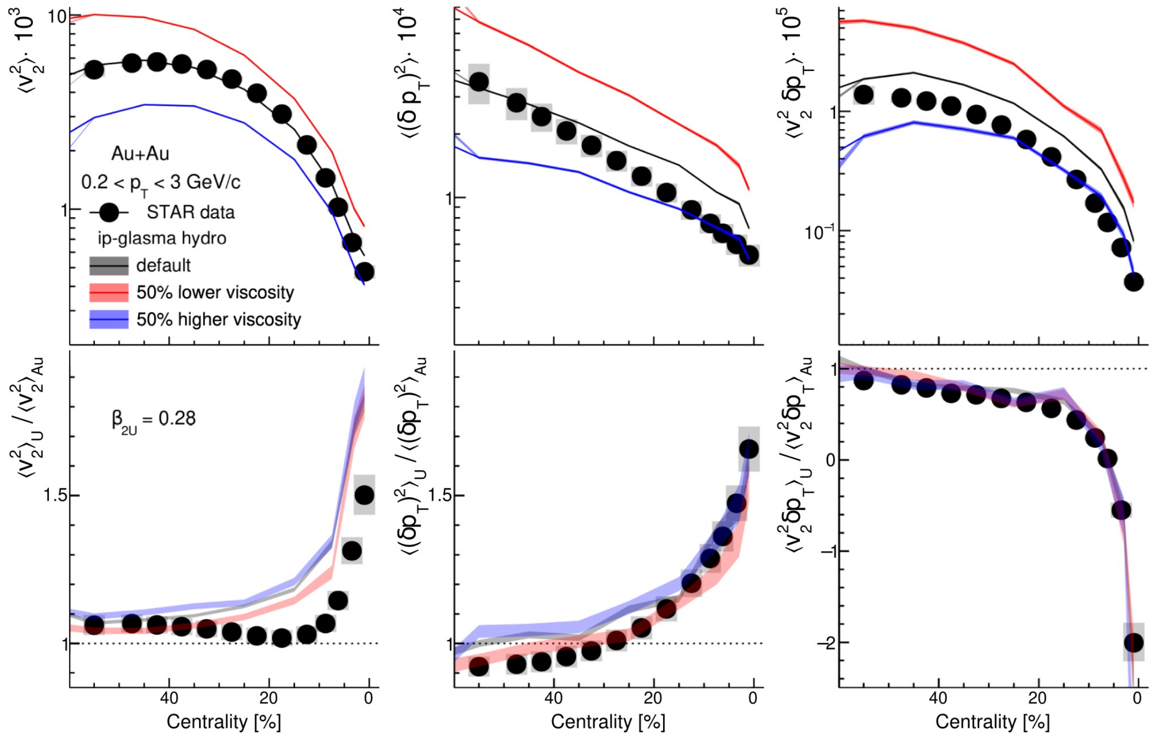

2) Effect from nuclear parameters are small, included as model systematics.

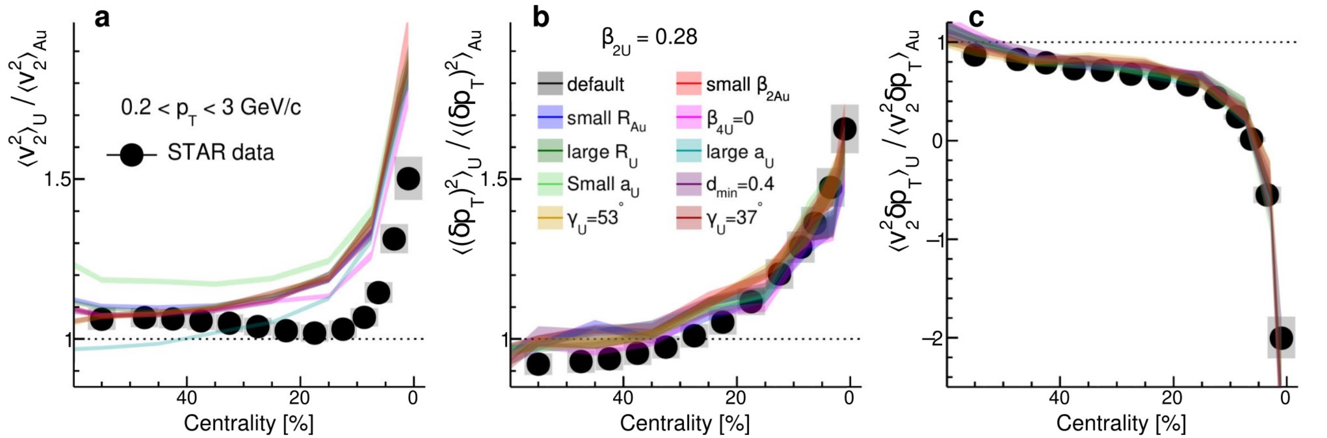

3) Another hydrodynamics model, Trajectum, shows rather consistent extractions even if it was not tuned to RHIC data.

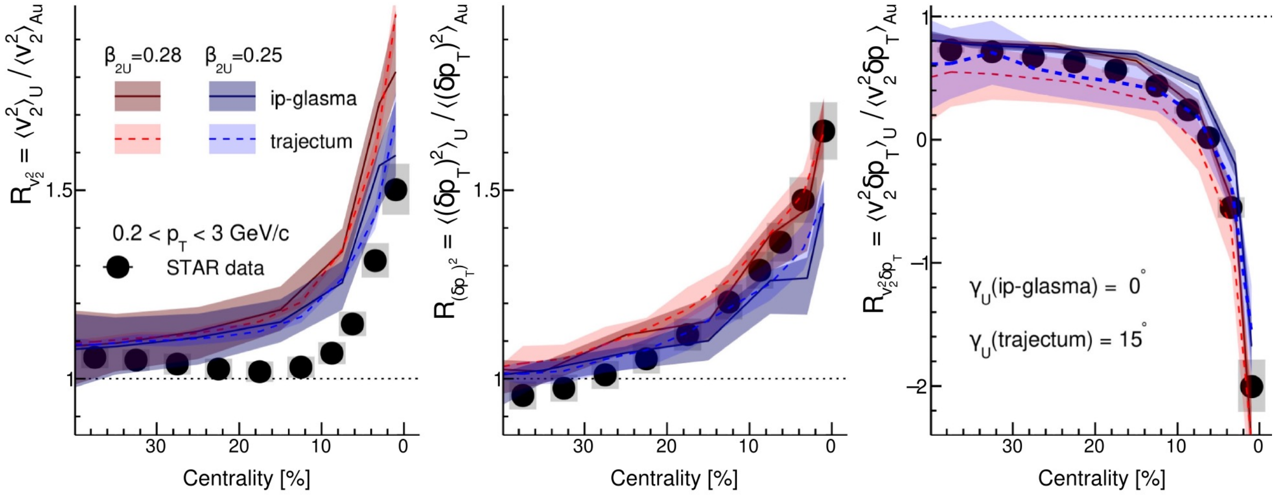

Extracted $\beta_{2,\mathrm{U}}$ and γ_{U} values are robust.

Nuclear structure is inherent of heavy-ion probes

one-body distribution | two-body correlations | three-body correlations

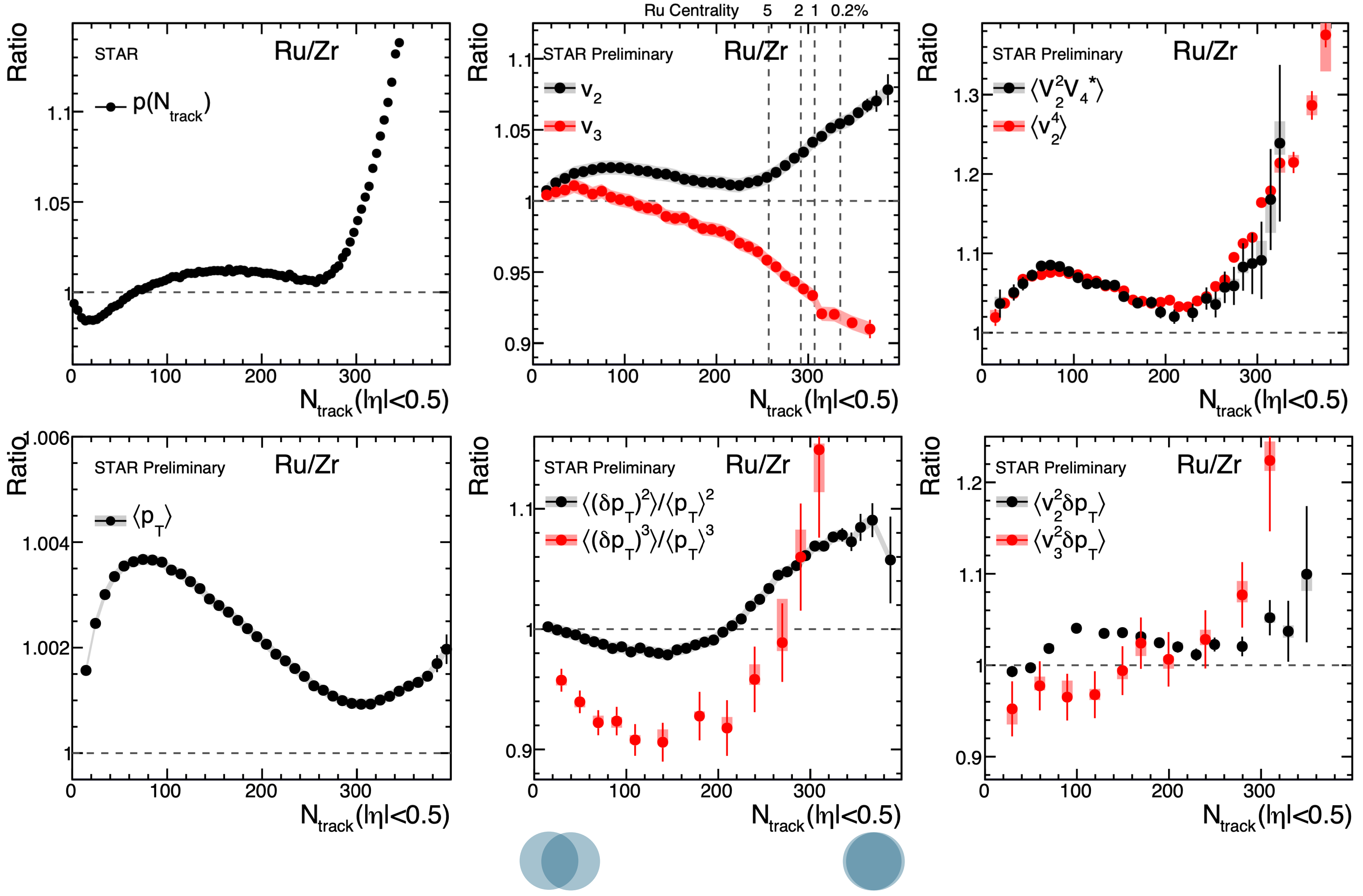

Linear response in ultra-central collisions

$$\frac{\delta[p_T]}{[p_T]} \propto -\frac{\delta R_\perp}{R_\perp}$$

$$V_n \propto \mathcal{E}_n$$

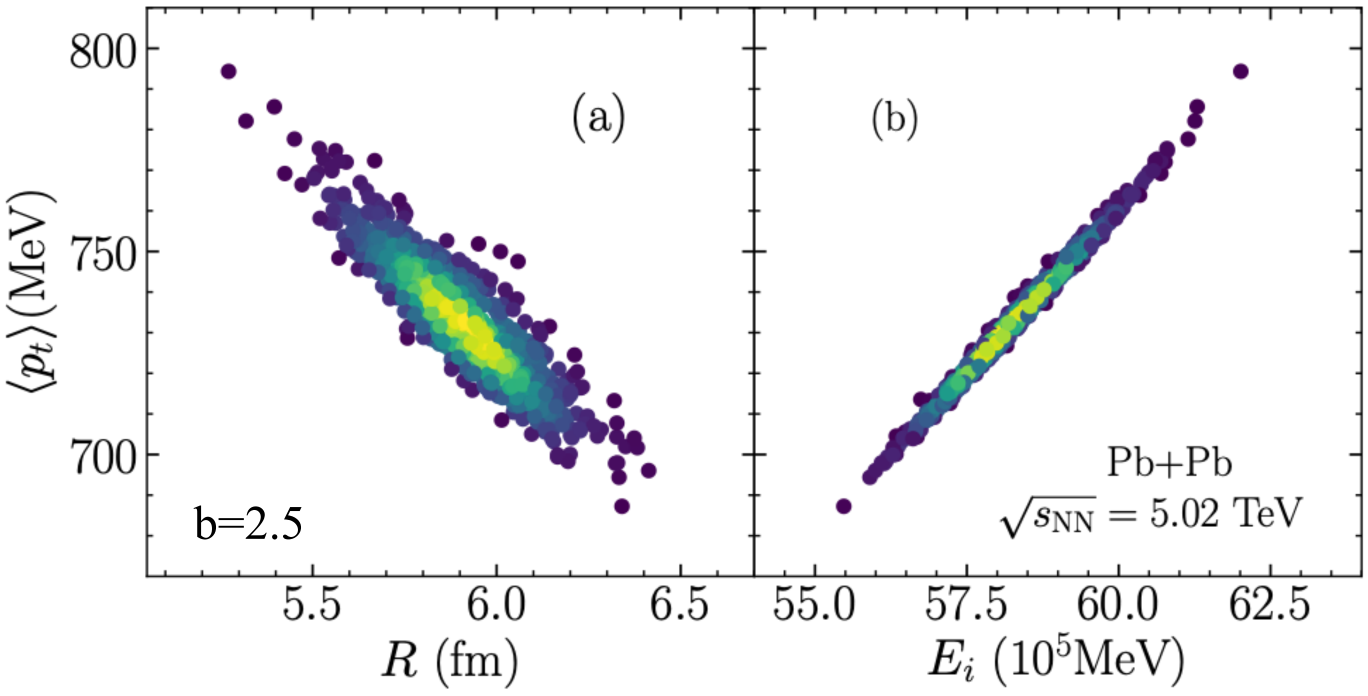

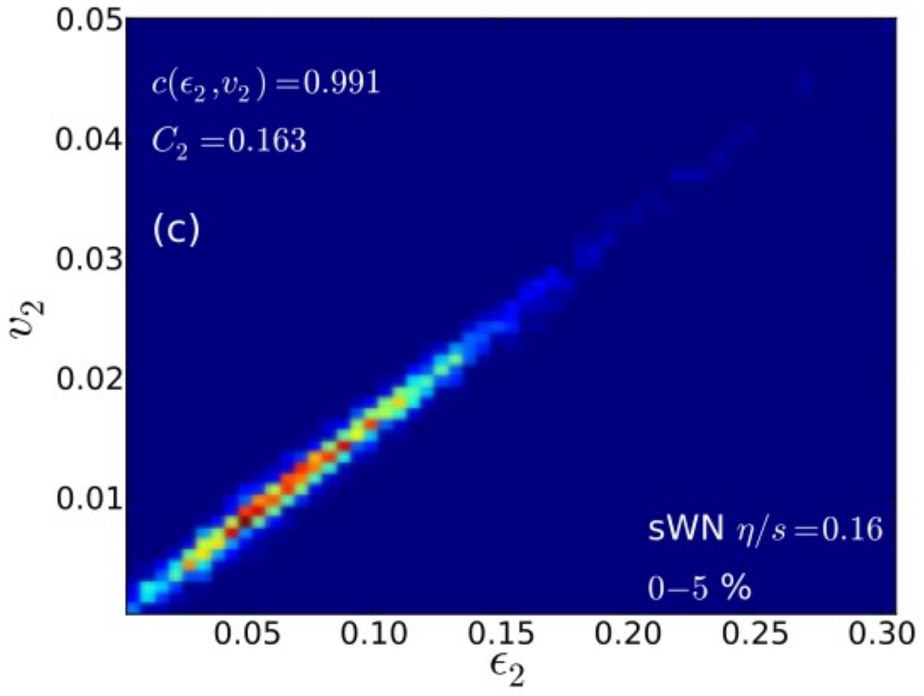

G. Giacalone, F. Gardim, J. Hostler, J. Ollitrault, et al, PRC 103, 024909 (2021)

H. Niemi, G. Denicol, H. Holopainen, P. Huovinen, PRC 87, 054901 (2013)

Probe $\beta_{3,\mathrm{U}}$ and its fluctuation

L. Liu, C. Zhang, J. Chen, J. Jia, X. Huang, Y. Ma, 2509.09376

Octupole collectivity

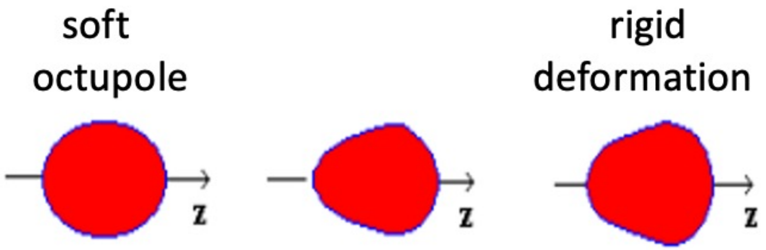

$$\langle \beta_3^2 \rangle = \bar{\beta}_3^2 + \sigma_{\beta_3}^2$$

$$c_{n,\varepsilon}\{2\} = \langle \varepsilon_n^2 \rangle \approx \langle \varepsilon_{n,0}^2 \rangle + \langle p_n p_n^* \rangle \underline{\langle \beta_n^2 \rangle}$$

$$c_{n,\varepsilon}\{4\} = \langle \varepsilon_n^4 \rangle - 2\langle \varepsilon_n^2 \rangle^2$$
$$\approx \langle \varepsilon_{n,0}^4 \rangle - 2\langle \varepsilon_{n,0}^2 \rangle^2 + \langle p_n^2 p_n^{2*} \rangle \underline{\langle \beta_n^4 \rangle} - 2\langle p_n p_n^* \rangle^2 \underline{\langle \beta_n^2 \rangle^2}$$

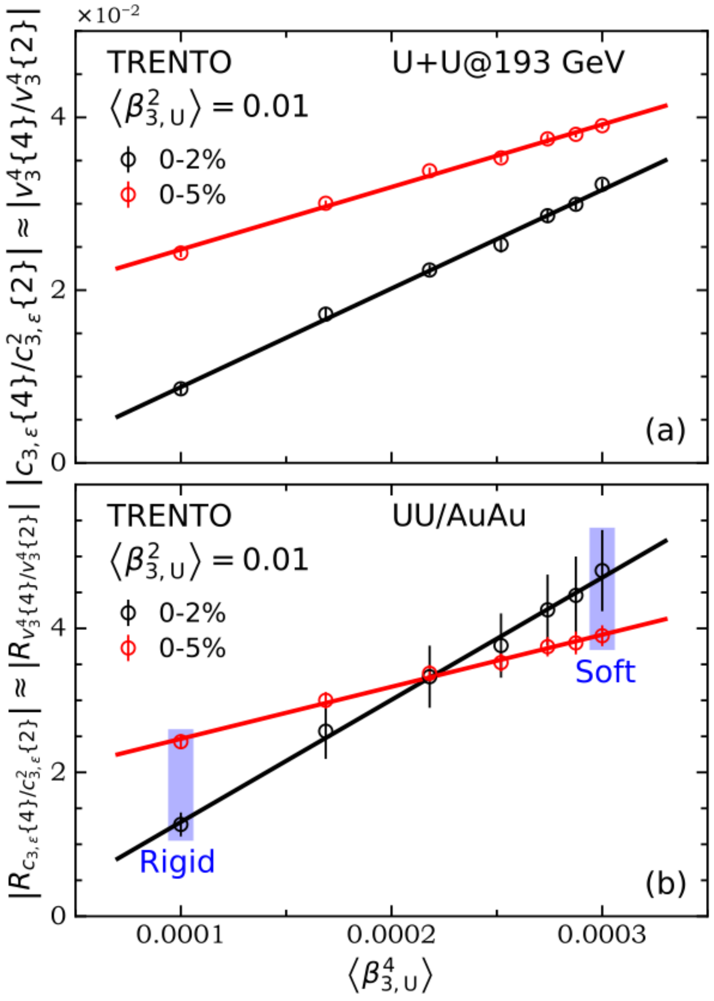

Four-particle correlation is linearly scaled to $\langle \beta_{3,\mathrm{U}}^4 \rangle$.

A way to discriminate between static and dynamic collective modes in high-energy nuclear collisions